NREL
NATIONAL RENEWABLE ENERGY LABORATORY

Laboratory Performance Testing of Residential Window Air Conditioners

J. Winkler, C. Booten, D. Christensen, and J. Tomerlin

NREL is a national laboratory of the U.S. Department of Energy, Office of Energy Efficiency & Renewable Energy, operated by the Alliance for Sustainable Energy, LLC.

Technical Report
NREL/TP-5500-57617
March 2013

Contract No. DE-AC36-08GO28308

NREL
NATIONAL RENEWABLE ENERGY LABORATORY

Laboratory Performance Testing of Residential Window Air Conditioners

J. Winkler, C. Booten, D. Christensen, and J. Tomerlin

Prepared under Task No. BE12.0201

National Renewable Energy Laboratory
15013 Denver West Parkway
Golden, Colorado 80401
303-275-3000 • www.nrel.gov

Technical Report
NREL/TP-5500-57617
March 2013

Contract No. DE-AC36-08GO28308

NOTICE

Available electronically at http://www.osti.gov/bridge

Available for a processing fee to U.S. Department of Energy
and its contractors, in paper, from:

U.S. Department of Energy
Office of Scientific and Technical Information
P.O. Box 62
Oak Ridge, TN 37831-0062
phone: 865.576.8401
fax: 865.576.5728
email: mailto:reports@adonis.osti.gov

Available for sale to the public, in paper, from:

U.S. Department of Commerce
National Technical Information Service
5285 Port Royal Road
Springfield, VA 22161
phone: 800.553.6847
fax: 703.605.6900
email: orders@ntis.fedworld.gov
online ordering: http://www.ntis.gov/help/ordermethods.aspx

Cover Photos: (left to right) PIX 16416, PIX 17423, PIX 16560, PIX 17613, PIX 17436, PIX 17721

Printed on paper containing at least 50% wastepaper, including 10% post consumer waste.

Executive Summary

Window air conditioners (ACs) are the dominant cooling product for residences, in terms of annual unit sales. They are inexpensive, portable, and can be installed by the owner. For these reasons, they are an attractive solution for supplemental cooling, for retrofitting air conditioning into a home that lacks ductwork, and for renters. Window ACs for sale in the United States are required to meet very modest minimum efficiency standards.

The Building America program is tasked with developing and demonstrating practical tools and strategies to cost-effectively retrofit existing buildings. We use annual simulation tools to evaluate the interactions of all building efficiency measures, and determine the resulting energy/cost tradeoffs and relative benefits of different retrofit strategies and technology improvements. To understand the relative benefits of replacing inefficient cooling systems, such as current window ACs, with a more efficient measure, we need accurate numerical models and data on specific units' performance. We also need a detailed understanding of the unintended impacts of a technology from a whole-building perspective; in the case of window ACs the primary unintended impact is a significant increase in building air infiltration that results from their installation in windows.

We tested four window ACs' performance in the National Renewable Energy Laboratory's Advanced Heating, Ventilation, and Air-Conditioning Systems Laboratory. The goal was to separate and study the refrigerant system performance, the internal leakage pathways, the fan-forced ventilation, the leakage around the units resulting from installation in a window, and the recirculation of supply air into the returns. To accomplish this we devised a series of tests that focused on each aspect of each unit's performance; selected results are shown below.

Window AC	Manufacturer-Rated Performance		Measured Performance	
	Capacity (Btu/h)	EER (Btu/Wh)	Capacity (Btu/h)	EER (Btu/Wh)
Frigidaire (FRA103BT1)	10,000	9.8	9,298	8.9
Frigidaire (FRA106CV1)	10,000	10.7	10,028	11.5
Haier	5,000	9.7	4,767	8.8
GE (old)	6,000	9.7	3,497	4.3

EER = energy efficiency ratio; GE = General Electric

Window Air Conditioner	Equivalent SEER (Btu/Wh)
Frigidaire (FRA103BT1)	9.3
Frigidaire (FRA106CV1)	12.1
Haier	9.9
GE (old)	4.7

SEER = seasonal energy efficiency ratio

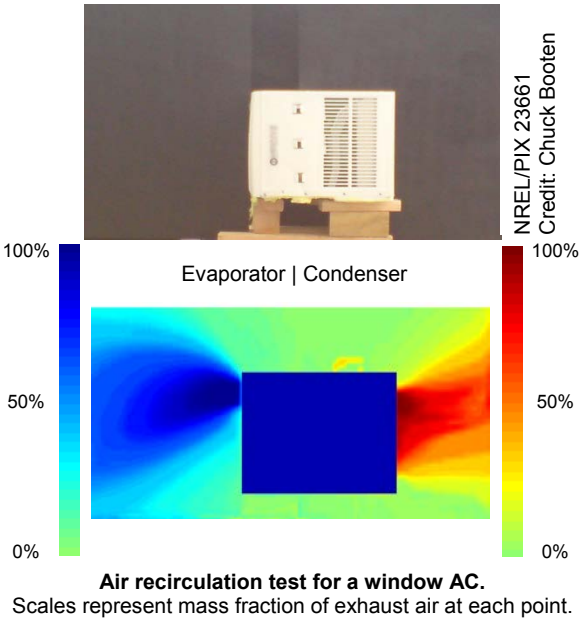

Air recirculation test for a window AC.
Scales represent mass fraction of exhaust air at each point.

These tests were designed to develop a detailed performance map to determine whole-house performance in different climates. Even though the test regimen deviated thoroughly from the

industry standard ratings test, our results permit simple calculation of an estimated rating for capacity and efficiency that would result from a standard ratings test. This calculation method revealed that the three new ACs' measured performance was consistent with their ratings.

We developed performance datasets across a broad range of indoor and outdoor operating conditions, and used them to generate performance maps. Performance maps are the sets of inputs necessary to simulate the products in an annual whole-building energy simulation. We also used the test data to characterize air leakage. Air leakage caused by the intended installation in a window, per manufacturer instructions, was surprisingly high.

There are many opportunities for improving installed performance of window ACs. The U.S. Department of Energy and U.S. Environmental Protection Agency[1] suggest the following as primary opportunities for improved energy efficiency:

- Using newer compressor technologies
- Increasing heat exchanger sizes or using micro-scale enhancements
- Improving fan blade designs or changing to a dual-fan design
- Reducing thermal bridging and internal air leakage
- Using heat pipes to enhance heat exchangers
- Improving weatherization through corrosion protection such as polymers or powder-coating components
- Increasing connectivity between packaged terminal air conditioning and the smart grid.

Based on the results of this study, several additional opportunities for improving the performance of window ACs, including those already installed in homes around the country, were identified and described.

Recommended Design Modification	Method to Achieve	Potential Performance Improvement
Reduce Installation Infiltration	• Provide better installation attachments such as closed-cell foam weather stripping, removable tape, and similar.	Infiltration reduced by up to 47 sq. in., or up to 90 cfm50[1]
Reduce Air Recirculation	• Invert the interior components so the evaporator supply is at the bottom. • Supply an attachment fin to separate supply and return airflows.	At least 1 EER
Reduce the Barriers to Excellent Maintenance	• Provide better air filters. • Provide an air filter for the condenser. • Provide a cage or grille to limit damage to condenser fins. • Provide a means to clean the refrigerant coils using a vacuum.	Up to 4 EER[2]
Increase Airflows	• Provide better fan blade design, including scalloped trailing edges.	At least 1 EER Lower noise

[1] cfm50 = cubic feet per minute at 50 Pa
[2] Proper and effective maintenance over the life the unit could prevent up to a 4 EER decrease

[1] See, for example: EPA (2011).

Definitions

AC	air conditioner
AHRI	Air-Conditioning, Heating, and Refrigeration Institute
ANSI	American National Standards Institute
ASHRAE	American Society of Heating, Refrigerating and Air-Conditioning Engineers
Btu	British thermal unit
C_D	degradation coefficient
cfm	cubic feet per minute
CLF	cooling load factor
COP	coefficient of performance
DB	dry-bulb
DOE	U.S. Department of Energy
DP	dew point
EER	energy efficiency ratio
EIR	energy input ratio
EPA	U.S. Environmental Protection Agency
EWB	entering wet-bulb
GE	General Electric, Inc.
HVAC	heating, ventilating, and air-conditioning
IR	infrared
LFE	laminar flow element
NREL	National Renewable Energy Laboratory
Pa	Pascal
PTAC	packaged terminal air conditioner
PTHP	packaged terminal heat pump
scfm	standard cubic feet per minute
SEER	seasonal energy efficiency ratio
SHR	sensible heat ratio
WB	wet-bulb

Contents

List of Figures

List of Tables

1 Overview

Four residential window air conditioners (ACs), a type of packaged terminal air conditioners (PTACs), were tested in the National Renewable Energy Laboratory's (NREL) Advanced Heating, Ventilating and Air Conditioning (HVAC) Systems Laboratory. Each unit underwent a series of tests across a wide range of operating conditions, to evaluate its operational efficiency, delivered capacity, air leakage, and other practical effects that would impact whole-house energy consumption and occupant comfort in a real-world setting.

Table 2 at the end of this section lists the test units along with their manufacturer-provided specifications. Three test units were purchased new. The fourth unit was obtained during an NREL-assisted hot-humid climate residential retrofit project. The owner/occupant determined this window AC had reached the end of its usable life, and was replacing it with a newer, more efficient unit. During the retrofit, NREL engineers retrieved the unit. It was then tested as closely as possible to the as-found condition to investigate whether its performance had degraded over its life, and if so by how much. Prior studies indicate the expected life of a window AC is 10 years (DOE 2008); the fourth test unit was 11 years old when taken out of service.

1.1 Motivation

The window AC is a common appliance for space cooling in older buildings across the United States, and to deliver supplemental cooling when central equipment does not meet occupant comfort requirements. Although renters are a perceived primary market for these ACs, these units also seem to be commonly used by homeowners to improve comfort in older buildings that lack ducted central systems, and in cases where a central system upgrade is first-cost prohibitive. To understand the energy/cost/comfort tradeoffs of window ACs, additional information is needed beyond the basic rating information and performance estimates that manufacturers occasionally provide. This report is the first step in understanding the relative benefits of replacing a home's window ACs with a more efficient cooling technology during a retrofit. Our results can also be used to perform more detailed and accurate studies in any region of the United States.

The window AC market in the United States is very large; in fact it is the dominant product for residential cooling in terms of unit sales.[2] American consumers spent $1.32 billion on more than 7.5 million units in 2011, with projected growth beyond 8.6 million units in 2015. Contrast those figures with the roughly 5.5 million ducted split ACs sold in 2011. Only 350,000 through-the-wall units were sold in 2011, roughly the same number as mini-splits. More than 95% of the window ACs sold are imported.

Window ACs and other packaged systems are rated using an energy efficiency ratio (EER) as defined by the Air-Conditioning, Heating, and Refrigeration Institute (AHRI) 310/380. This standard was adopted by the U.S. Department of Energy (DOE) into the Code of Federal Regulations (CFR) for enforcement of minimum efficiency standards. Window ACs are typically sized at 6,000–16,000 Btu/h (0.5-1.3 tons, or 1750–4700 kW of cooling) and many incorporate

[2] All market statistics in this paragraph are sourced from BSRIA (2012)

resistance heaters to provide year-round comfort. Systems with refrigerant reversing valves, known as packaged terminal heat pumps (PTHPs), can provide more efficient space heating and occupy roughly half of the residential PTAC/PTHP market (DOE 2008).[3] Heating mode efficiency for PTHPs is characterized by a coefficient of performance (COP). Table 1 summarizes federal efficiency minimums for PTACs and PTHPs as of this report's publication date (DOE 2013).

Table 1. Current Federal Minimum Efficiency Standards

Equipment	Cooling Capacity (Btu/h)	Existing Federal Minimum Efficiency Standard	
		EER [1]	COP
PTAC	< 7,000	8.88	N/A
	7,000 to 15,000	10.0 - (0.16 × Cap)	
	> 15,000	7.6	
PTHP	< 7,000	8.88	2.7
	7,000 to 15,000	10.0 - (0.16 × Cap)	1.3 + (0.16 × EER)
	> 15,000	7.6	2.5

[1] "Cap" means capacity in kBtu/h at standard test conditions

Although PTACs are evaluated using a different metric than unitary split ACs, they are overall much less efficient than split systems. However, window AC cost is an order of magnitude lower than the cost of installing a central cooling system. Thus, life cycle cost analysis indicates that many years of efficient energy consumption are likely needed for a central HVAC system to compete on a cost basis with a window AC. This laboratory study was performed in part to inform follow-on research to evaluate if and when window ACs are a cost-effective HVAC solution, and what whole-home system interactions result from their use.

Most window ACs can be installed either in a window or more permanently in a framed wall opening (depending on the design of the condenser side vents). The AHRI 310/380 standard test method is reasonable for representing a through-wall installation, where the equipment case can be well-sealed into a close-fitting sleeve. In contrast, operable windows exist in many sizes and construction types. Window AC manufacturers provide inexpensive attachments for use in window installations. The integrated performance of window units is not considered in the current rating, yet may cause real-world performance to deviate significantly from the rated efficiency.

1.2 Experiment Summary

To evaluate the expected impacts of real-world window installations, we performed a series of tests to disaggregate and characterize different mechanisms for efficiency loss. Those mechanisms include:

- Increase in whole-home natural infiltration (incremental air leakage)
- Forced infiltration driven by window AC unit operation (unintended ventilation)

[3] This report focuses on window ACs only, but PTHP information is included here for completeness. We believe this report's significant conclusions and recommendations for performance improvement apply equally to both classes of equipment.

- Refrigerant system operational efficiency (actual cycle performance)
- Air recirculation from supply to return on both indoor and outdoor sides (increase in required temperature lift).

We first studied the air infiltration increase resulting from window AC use by constructing a plenum containing two residential operable windows of different widths, and characterized its leakage with the windows closed. We installed each test unit following manufacturer instructions, and characterized the change in plenum leakage caused by the window AC. Next, we placed a plastic liner across the window and sealed it to the wall and the AC case exterior. Leakage under this condition can be attributed to air pathways through the unit, and can be used to estimate infiltration for a through-wall installation. The method used in this experiment was analogous to a whole-home blower door test.

To measure fan-driven ventilation, we operated the units in each fan setting and measured airflow into or out of the plenum over a range of pressures relative to ambient. This experiment was analogous to using a powered flow hood to measure register airflows.

We then temporarily removed the case of each unit and air sealed each one's interior to the fullest extent possible. After installing power measurement instrumentation, we reassembled the cases and enclosed each window AC in an insulated plenum that separated inlet (return) airflows from outlet (supply) airflows. This allowed us to independently control pressures to minimize air leakage through whatever pathways remained, and to accurately measure energy and mass flows. We tested each window AC across a wide range of indoor and outdoor operating temperatures. This experiment was analogous to the standard test method for unitary split air conditioners.

Finally, we removed each AC from its insulated plenum and operated it in free air, with a calibrated screen that allowed us to perform thermal imaging and airflow measurements. These data were used as input to a MATLAB image processing routine to calculate an overall air recirculation fraction for both indoor and outdoor sides of each window AC. Recirculation results in a colder, dryer inlet condition to the indoor (evaporator) coil, and a hotter inlet condition to the outdoor (condenser) coil. It will therefore reduce operating efficiency and cooling capacity.

There are many opportunities for improving the installed performance of window air conditioners. DOE and the U.S. Environmental Protection Agency (EPA)[4] suggest the following as primary opportunities for improved energy efficiency:

- Using newer compressor technologies
- Increasing heat exchanger sizes or using micro-scale enhancements
- Improving fan blade designs or changing to a dual-fan design
- Reducing thermal bridging and reducing internal air leakage
- Using heat pipes to enhance heat exchangers

[4] See, for example: EPA (2011).

- Improving weatherization through corrosion protection such as polymers or powder-coating components
- Increasing connectivity between the PTAC and the smart grid.

The results of this study showed several additional opportunities for system performance improvement that are extremely inexpensive, low-tech, and require minimal innovation or manufacturer action. Nearly all these recommendations can be easily applied to cost-effectively retrofit window ACs already installed in U.S. homes. We summarize those opportunities at the end of this report.

The four test units and their rated performance are listed in Table 2. The General Electric (GE) unit had been installed and used in the field for 11 years. In the southern United States and Hawaii, these units are often left in place continuously for years because of year-round cooling demand. Examining a unit that has undergone such extensive use provides good insights into the potential for performance improvements. A detailed description of the unit and its installation is given in Appendix A.

Table 2. Window AC Test Unit Specifications

Brand Name	Model #	Capacity[1] (kBtu/h)	EER[1] (Btu/Wh)	Airflow Rate[2] (cfm)	ENERGY STAR® Qualified	Date of Manufacture
Frigidaire	FRA103BT1	10	9.8	231/260/290	No	11/2011
Frigidaire	FRA106CV1	10	10.7	231/260/290	Yes	10/2011
Haier	HWR-5XCL	5	9.7	115/125/135	No	Unknown[4]
GE	AGD06LAG1	6	9.7	N/A[3]	No	02/2001

[1] Performance at the rated return condition of 80°F (26.7°C) dry-bulb, 67°F (19.4°C) wet-bulb, and outdoor condition of 95F (35°C).
[2] Airflow rates correspond to low, medium, and high fan speeds, respectively, when available.
[3] Rated airflow rate data were not available for this unit because of its age.
[4] This unit did not have a nameplate to identify manufacture date. It is likely of recent manufacture, as it was purchased at a local big box store where product turnover is high.

2 Window Infiltration Testing

Two infiltration paths are attributed to window AC installation—through the unit, and the combination of all leaks between the case and the window frame. Both paths lead to added energy use by adding an additional infiltration load onto the AC. The leakage around the unit is the dominant contributor to infiltration and was investigated by installing each unit in a window and testing for leakage.

2.1 Test Method

Figure 1 shows a schematic of the test plenum that consisted of a carefully sealed and framed plywood box, sized approximately 4 ft × 8 ft × 8 ft. One wall included two residential single-hung windows (see Figure 2). A variable-speed blower was plumbed into the plenum through a laminar flow element (LFE) flow meter to create controllable pressures and measure airflows into and out of the chamber. Differential pressure across the chamber walls was measured via distributed pressure taps. The powered flow setup is shown in Figure 3.

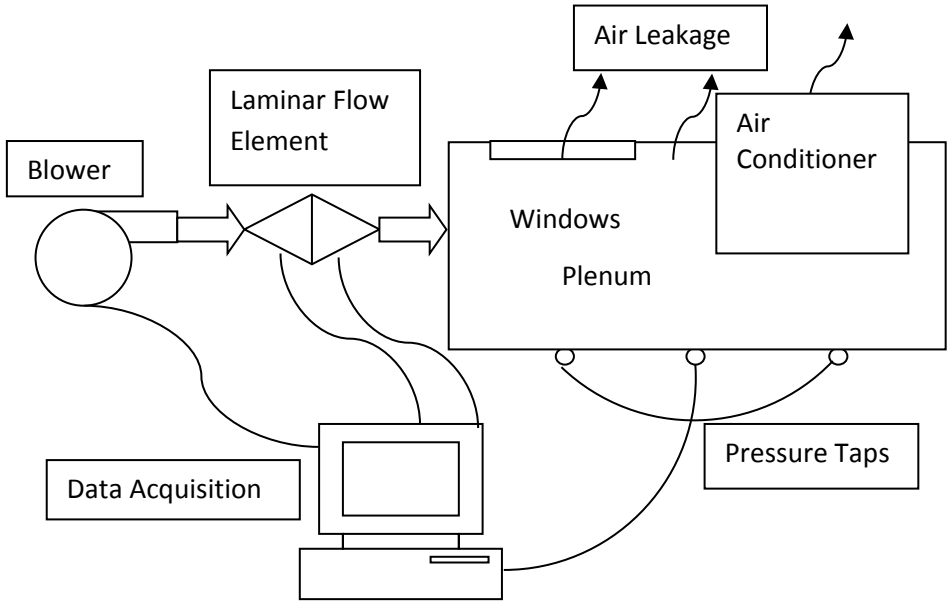

Figure 1. Infiltration test apparatus schematic

NREL/PIX 23655
Credit: Chuck Booten, NREL

Figure 2. Test chamber used to determine air leakage around and through each window AC

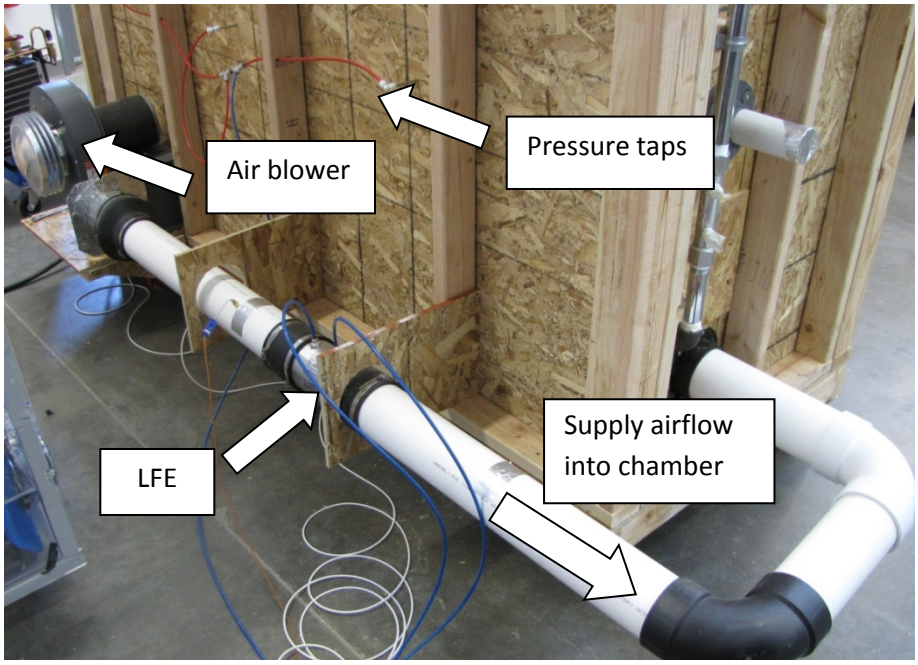

NREL/PIX 23656
Credit: Chuck Booten, NREL

Figure 3. Infiltration testing fan and sensors used to measure leakage airflow rate

Differential pressures between the chamber and ambient were applied between 0 and 50 Pa with the entire chamber sealed, and flows measured at each step, similar to a blower door test of a building. Pressures were incremented between 2 and 10 Pa with smaller steps at lower pressures. This baseline chamber leakage rate was subtracted from later leakage measurements to fairly attribute incremental infiltration to the window AC and related installation pathways.

AC unit leakage testing occurred in three steps:

1. Unit off, installed per manufacturer instructions—to understand the change in whole-home infiltration while the unit is installed but not operating.
2. Unit on, installed per manufacturer instructions—to understand the difference in whole-home infiltration while the unit is operating.
3. Unit on, case exterior sealed to plenum—to understand the fan-induced infiltration and case infiltration, separate from the installation effects.

The difference in leakage between these tests can be used to characterize opportunities for improvement.

Example setups are shown in Figure 4. The picture on the left is the setup used to determine the air leakage through the unit by air sealing all leakage paths caused by the installation.

NREL/PIX 23657 (left), 23658 (right)
Credit: Chuck Booten, NREL

Figure 4. Example test configuration. Left: All leakage eliminated except through the unit. Right: Using only factory-supplied materials for sealing per manufacturer instructions.

Leakage was measured at multiple pressures between 0 and 50 Pa. A least-squares curve fit of the form

$$Flow = A + BP^{0.5} + CP \quad (1)$$

where *A, B* and *C* are the fitted coefficients and *P* is the differential pressure in the chamber, was then used to compare leakage continuously over the entire pressure range. R-squared values were typically above 0.98. This form was used because viscous dominated flow regimes have a linear relationship between pressure and flow, and in inertial dominated flow regimes the flow is approximately proportional to the square root of pressure.

2.2 Test Results

The results are presented below for both Frigidaire units and the Haier unit. The leakage through the unit interiors (see Figure 5) relates to an installation similar to the left photo in Figure 4. The leakage is fairly modest at 0 Pa, 1–2 scfm increasing to 18–26 scfm at 50 Pa. There is no noticeable difference between the two Frigidaire units; however, both are significantly leakier than the Haier unit. The Frigidaire units have much larger capacity and physical size, so this is not surprising.

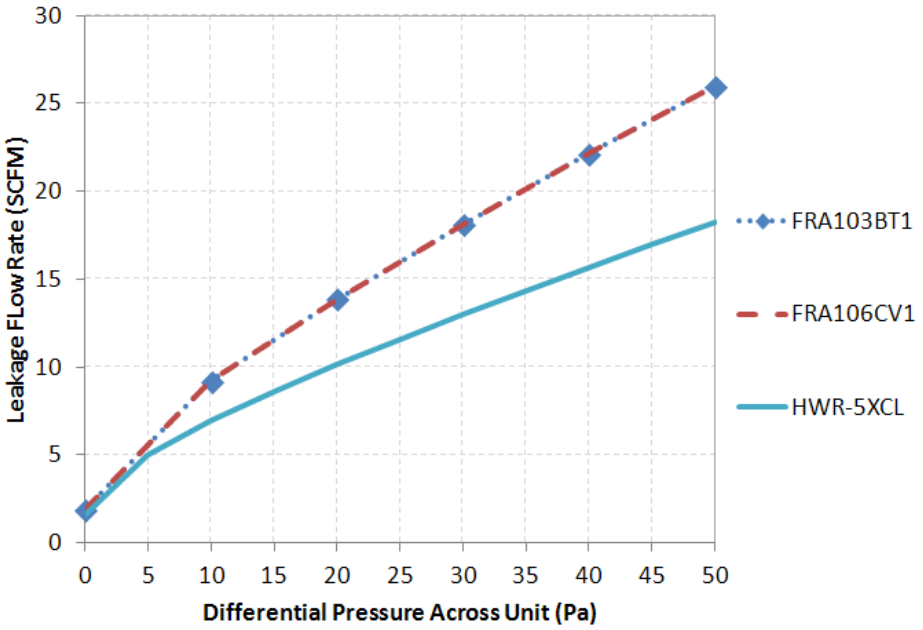

Figure 5. Leakage rate through each unit (traces are coincident for the Frigidaire units)

Most of the observed leakage was due to the installation effects, i.e. leakage through air pathways between the AC case and the window frame (see Figure 6), which corresponds to an installation similar to the right photo in Figure 4. In this test the window was "sealed" per manufacturer-supplied materials and instructions. The gaps were too large for these materials to seal well, except between the fixed and the hung sashes. This was essentially the worst-case installation scenario—leakage was increased by approximately 400%–500% over the well-sealed installation. This is equivalent to adding a 27–42 $in.^2$ hole in the wall. The primary driver of this

leakage is the louvers on either side of the unit. These louvers do not seal to the window frame on their own even if properly installed and are difficult to seal using tape or similar methods. The louvers are not required for structural integrity or safety. The air leakage can be significantly improved and can approach the leakage through the interior of the unit by not installing (or removing if already installed) the louvers, and using alternate means to better fill the gaps. Other materials such as plywood or foam can be cut to fit, then secured and sealed using a variety of inexpensive techniques such as taping the perimeter. Material costs of $5–$10 and 10–30 min for installation are reasonable for this effort.

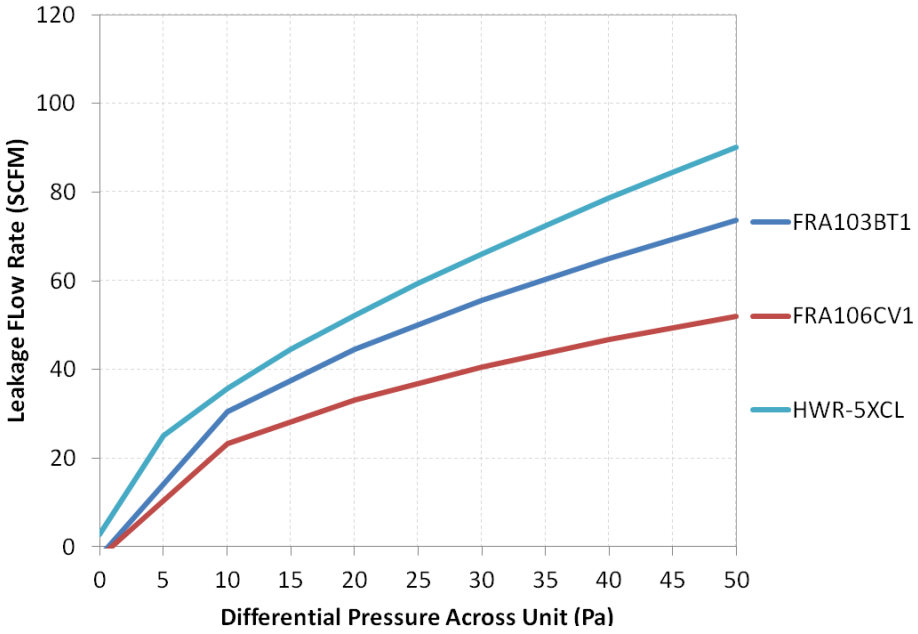

Figure 6. Leakage airflow rate exterior to the unit caused by installation

3 Airflow Recirculation Testing

The evaporator and condenser inlets and outlets are close to each other, so some of the air exiting both refrigerant coils becomes entrained in the return air and is recirculated into the respective inlets. This recirculation reduces the capacity and efficiency of the unit. The amount of recirculated air was measured and taken into account when developing the performance maps presented in Section 4. ASHRAE test method (ASHRAE 2009), which is used for rating units implicitly accounts for this recirculation. The delivered cooling and heating to the indoor and outdoor areas, respectively, are measured; any recirculated air simply reduces the efficiency and capacity of the unit. That method does not provide any information about the nature of any recirculation or whether it is even present. The information and the measurement technique used here have potential for improving the external airflow and design of future window ACs to increase performance at a potentially very low cost.[5]

3.1 Testing and Analysis

Tests were conducted using an infrared (IR) camera to image the supply and discharge temperatures of the evaporator and condenser. Two orientations are required to capture all airflows—one image from above the unit, which captured horizontal air movement and one from the side, which captured vertical air movement. An example of the imaging setup is shown in Figure 7.

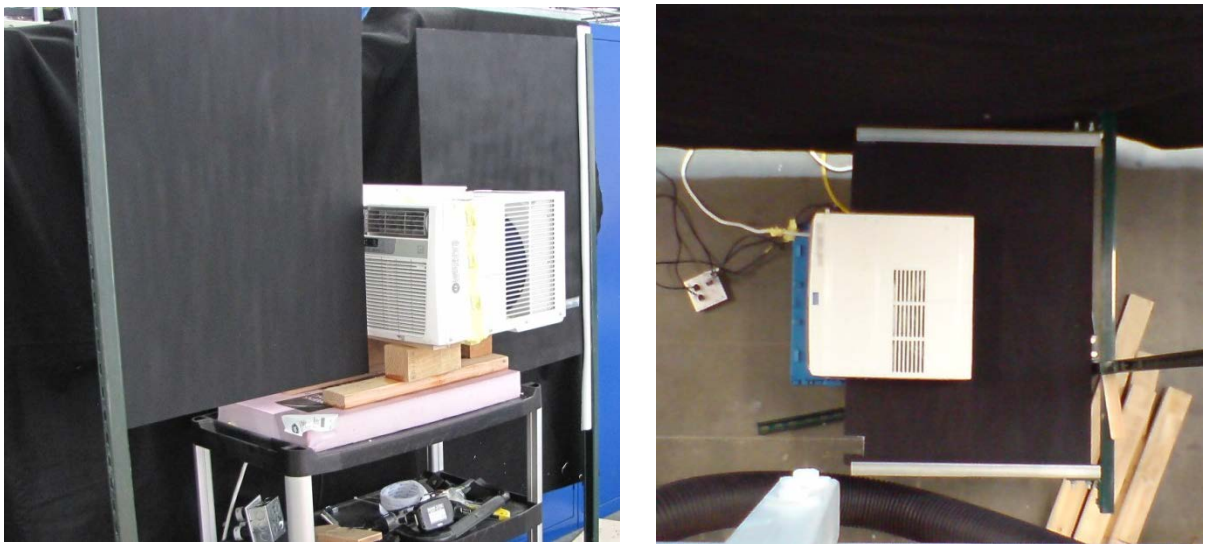

NREL/PIX 23659 (left), 23660 (right)
Credit: Chuck Booten, NREL

Figure 7. IR imaging test apparatus for imaging from the side (left) and from above (right)

The condenser and evaporator were imaged simultaneously using a FLIR SC660 camera programmed to save an image every 10 s. A single horizontal and a single vertical plane were selected as representative of the entire unit. Only the condenser is of interest in the horizontal image because condenser return registers are on the sides of the unit. The vertical image plane is

[5] An alternate method to measure air recirculation, with potentially greater accuracy, is to use particle image velicometry. This measurement method was unavailable to us, and we are collaborating with colleagues at the National Institute of Standards and Technology to verify and validate our method and results.

set by the location of the vertical black sheets placed approximately in the center of the unit horizontally. The sheets are poster board painted with Krylon #1602 paint, which has very well characterized optical properties that make it ideal for thermal imaging (Touloukian et al. 1972, Booten 2006). The poster board is composed of a foam core (~0.15 in. thick) with a cardboard facing (~0.02 in. thick). The horizontal orientation uses the same poster board but is imaged from above.

Steady state was determined after the test by comparing the images manually. Each unit was tested by first turning the unit on in fan-only mode and allowing it to achieve steady state. Approximately 30 images were then taken and averaged to form a reference image. The unit was then put in cooling mode and allowed to come to steady state at the high and low fan settings.

The velocity profiles at each inlet for the evaporator and condenser were measured using a hotwire anemometer. Velocity was measured at several locations at the same plane where the IR images are taken. Linear interpolation was used to estimate the full velocity profile.

The analysis used was an iterative solution of a conjugate heat transfer problem using finite volume discretization. This analysis is an example of an inverse heat conduction problem. This particular experimental and analytical technique was developed at NREL and is described in more detail in a separate report (Booten et al. 2013).

3.2 Results

The IR images at steady state are averaged to form a composite image of each unit at a reference condition and a high and low fan power while cooling. An example of a single image for the Frigidaire FRA106CV1 is shown in Figure 8. The composite reference image is subtracted from the operational images to give a net temperature difference shown in Figure 8. Examples from the images taken above the same unit are shown in Figure 9. These temperature distributions are used in the conjugate heat transfer solution to determine the true local air temperatures. The images of the horizontal plane, such as Figure 9, show asymmetry in the flow on the condenser. This leads to uncertainty about whether a single plane is sufficient for drawing conclusions about condenser recirculation. Given that the recirculation levels are so low and the uncertainty is approximately the same as the measured recirculation, the appropriate conclusion is that recirculation on the condenser does not have a significant impact on the unit's performance. Any recirculation caused by asymmetry that was out of the measurement plane is unlikely to be large enough to change that conclusion or result in recommended design changes to improve performance.

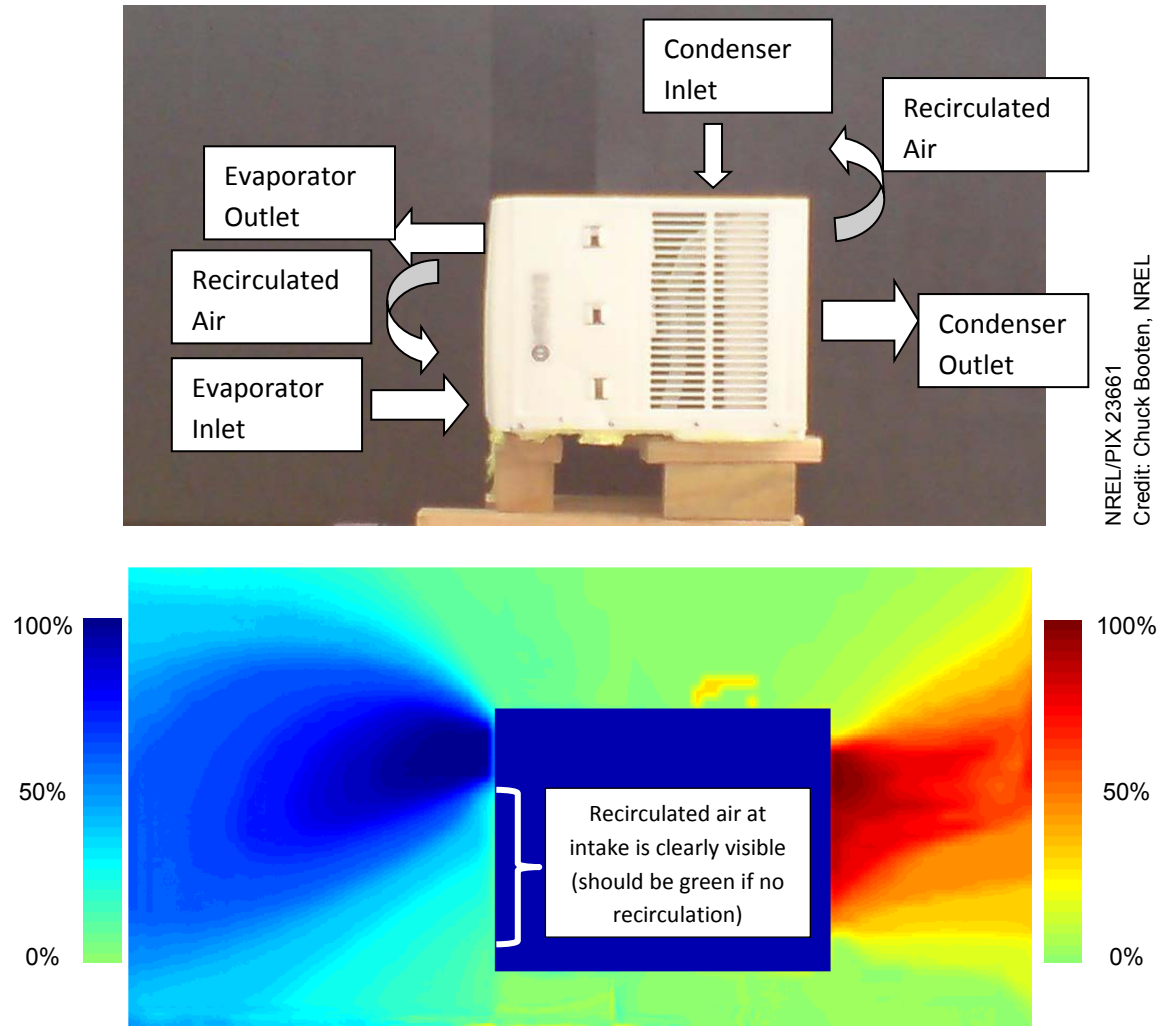

Figure 8. Example image of Frigidaire FRA106CV1 imaged from the side (top). The lower image shows calculated mixed air mass fraction of supply air at that location. The recirculation of the evaporator supply air is clearly visible. The thermal image was rescaled separately over the evaporator and condenser domains to represent the mass fraction of supply (outlet) air.

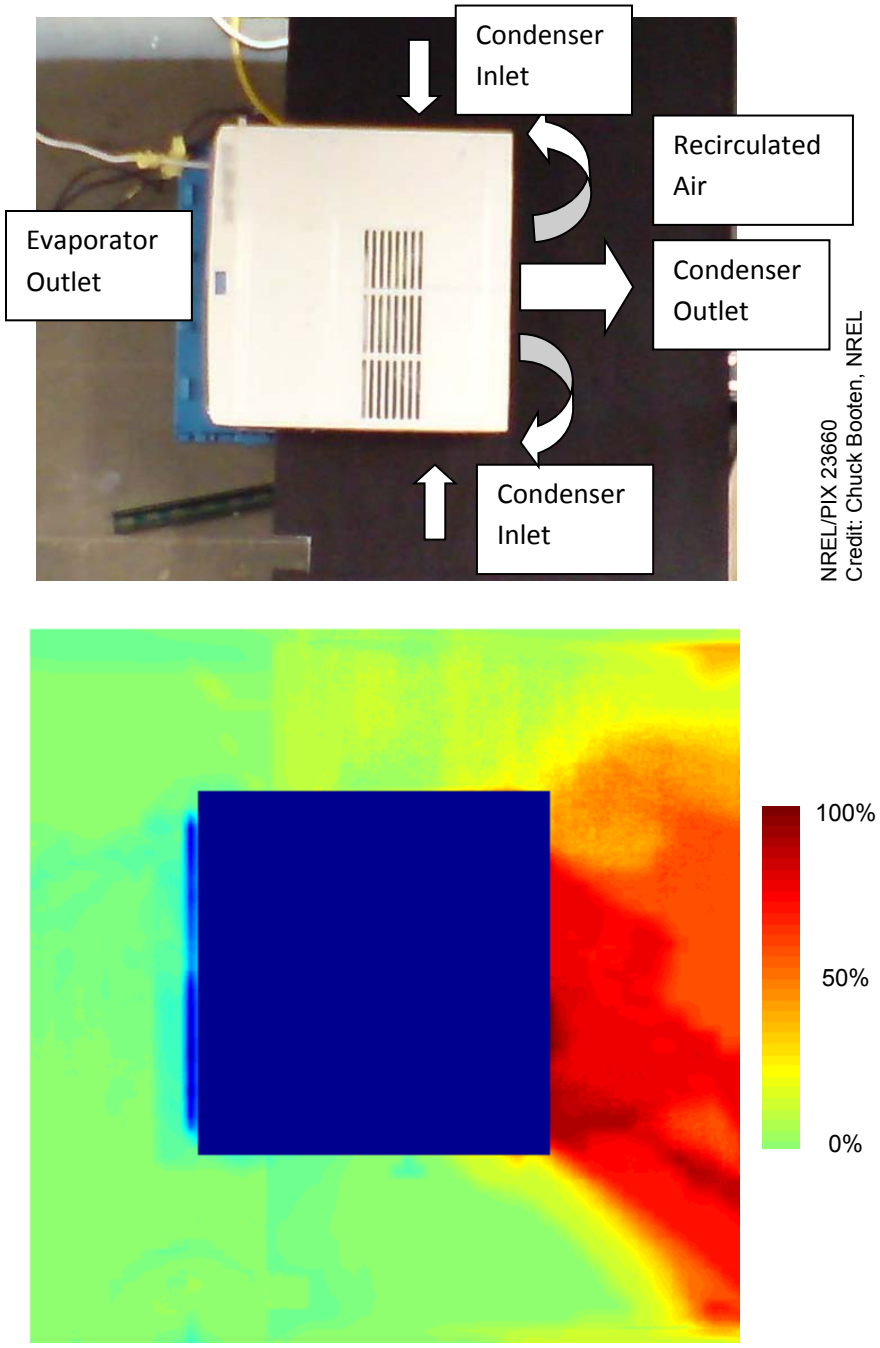

Figure 9. Example image of Frigidaire FRA106CV1 imaged from the top (photo). The lower image shows calculated mixed air mass fraction of condenser exhaust air at that location. The condenser outlet was not symmetric because of the shape of the fan shroud.

The recirculation percentages for the four units are given in Table 3. The evaporators were tested on low and high fan power because of the relatively large recirculation; however, the condensers were tested at low fan power only.

Table 3. Evaporator and Condenser Air Recirculation Mass Fractions

Brand Name	Model #	Evaporator (%)			Condenser (%)	
		Low	High	Uncertainty	Typical	Uncertainty
Frigidaire	FRA103BT1	22	26	2.0	4.0	2.7
Frigidaire	FRA106CV1	19	20	3.5	4.0	2.7
Haier	HWR-5XCL	28	22	2.8	-	3.5
GE (old)	AGD06LAG1	26.8	23.7	5.1	11.2	1.3

4 Window Air Conditioner Performance Testing

As in central systems, the compressor in a window AC cycles on and off to meet and maintain indoor air at the indoor temperature set point. This cycling degrades the operational efficiency compared to steady-state operation. In all window ACs, the condensate drains to the outdoor side of the unit, where it accumulates beneath the condenser before flowing out of the case and onto the ground. In two test units, the condenser fan blade passes through the accumulated condensate and sprays a small amount of condensate onto the condenser.[6] Thus, cyclic tests and tests to determine the impact of condensate injection were performed in addition to testing the four window ACs under steady-state operation.

This section describes the steady-state performance tests, cyclic tests, and the impact of the condensate spray. Because cyclic tests were performed, estimates of the seasonal energy efficiency ratio (SEER) were also made.

4.1 Test Setup

The test procedure specified in ASHRAE Standard 16-1983 is based on the use of calorimetric chambers (ASHRAE 2009). The Advanced HVAC Laboratory's configuration uses a highly calibrated flow loop to achieve heat and mass balances across a control volume. A calibrated flow loop makes it possible to conduct steady-state and cyclic performance tests very rapidly across a wide range of operating conditions, thereby developing robust data necessary to predict system performance under actual operating conditions in different climates.

LFEs (Figure 10) were used to measure evaporator and condenser inlet and outlet airflow rates. For both Frigidaire units, calibrated nozzles were used to measure the condenser inlet and outlet flow rates caused by the excessive pressure drop through the LFE. An air mass balance was calculated throughout testing to ensure the total air mass entering the unit was equal to the exiting air mass, within the expected uncertainty of about 2%. Three mass balances were calculated—an evaporator mass balance, condenser mass balance, and total mass balance—to ensure air was not being exchanged between the evaporator and condenser sides of the AC.

$$\varepsilon_{M,evap} = \frac{\dot{m}_{evap,in}}{\dot{m}_{evap,out}} \tag{2}$$

$$\varepsilon_{M,cond} = \frac{\dot{m}_{cond,in}}{\dot{m}_{cond,out}} \tag{3}$$

$$\varepsilon_{M,total} = \frac{\dot{m}_{evap,in} + \dot{m}_{cond,in}}{\dot{m}_{evap,out} + \dot{m}_{cond,out}} \tag{4}$$

[6] We believe this is a common practice for improving EER, and is likely found on most ENERGY STAR-rated window ACs.

Chilled mirror hygrometers (Figure 10), with an accuracy of ±0.36°F (±0.2°C), were used to measure the condenser and evaporator inlet and outlet dew point (DP) temperatures. A coriolis mass flow meter was used to measure condensate drain mass flow rate. A moisture mass balance (ε_{water}) was defined as the ratio of instantaneous inlet air moisture mass flow rate to the sum of outlet air moisture mass flow rate and condensate flow rate. Condensate was drained from below the evaporator, flow measured, and reintroduced into the condenser drain pan. Several of the test units' condenser fans are designed to pick up water from the condenser pan and induce a spray of water onto the condenser to improve efficiency. The condensate spray mass flow rate could not be measured, thus a moisture balance could only be determined on the evaporator side.

$$\varepsilon_W = \frac{\dot{m}_{evap,in} w_{evap,in}}{\dot{m}_{evap,out} w_{evap,out} + \dot{m}_{condensate}} \quad (5)$$

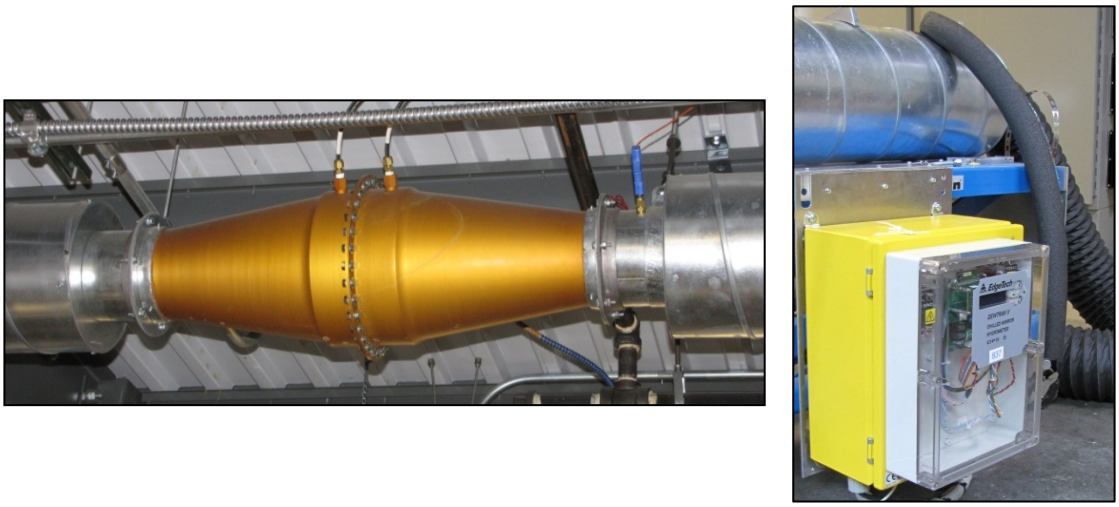

NREL/PIX 18679 (left), 21468 (right)
Credit: Bethany Sparn

Figure 10. LFE (left), used to measure airflow rate, and chilled mirror hygrometer (right) for DP measurements

A thermocouple array in the ductwork near the unit was used to measure well-mixed inlet and outlet temperatures. Static pressure was measured at the inlet and outlet. Standard ASHRAE formulas were used to calculate enthalpy for each air stream. Total unit power and fan power were individually measured using two power meters. An energy balance (ε_{energy}) was defined as the ratio of the sum of inlet air energy rate and electric power to the outlet air energy rate.

$$\varepsilon_{Energy} = \frac{\dot{m}_{evap,in} h_{evap,in} + \dot{m}_{cond,in} h_{cond,in} + \dot{P}_{total}}{\dot{m}_{evap,out} h_{evap,out} + \dot{m}_{cond,out} h_{cond,out}} \quad (6)$$

4.1.1 Plenum Construction and Air Sealing

Plenums for the test articles were constructed using 2-in. rigid insulation foam board, giving the plenums an R-value of approximately 13. Spacing around the test article was sufficient to allow even distribution of the conditioned air supplied by the laboratory, without impinging on any one certain point of the test article. The plenum was sealed internally and externally using 4 mil aluminum foil tape and expanding foam where needed. Based on airflow requirements, 6-in. duct

flanges were sealed to the plenum to provide connection points to the laboratory airstreams. Two pressure taps were installed per chamber and each pair of taps was then averaged by connecting equal length tubing to each and joining the pairs of tubes into a single tube for measurement. Figure 11 through Figure 14 show the plenum construction.

NREL/PIX 23662
Credit: Jeff Tomerlin, NREL

Figure 11. The center section of the plenum construction, along with the air deflector for the outdoor air return

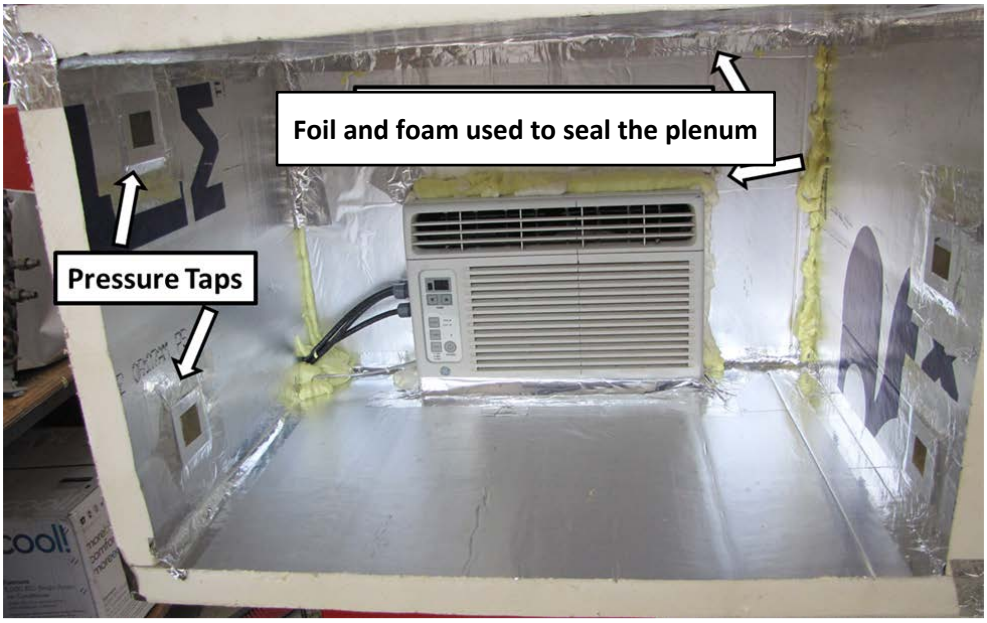

NREL/PIX 23663
Credit: Jeff Tomerlin, NREL

Figure 12. Front of the test unit sealed in plenum with foil tape and expanding foam

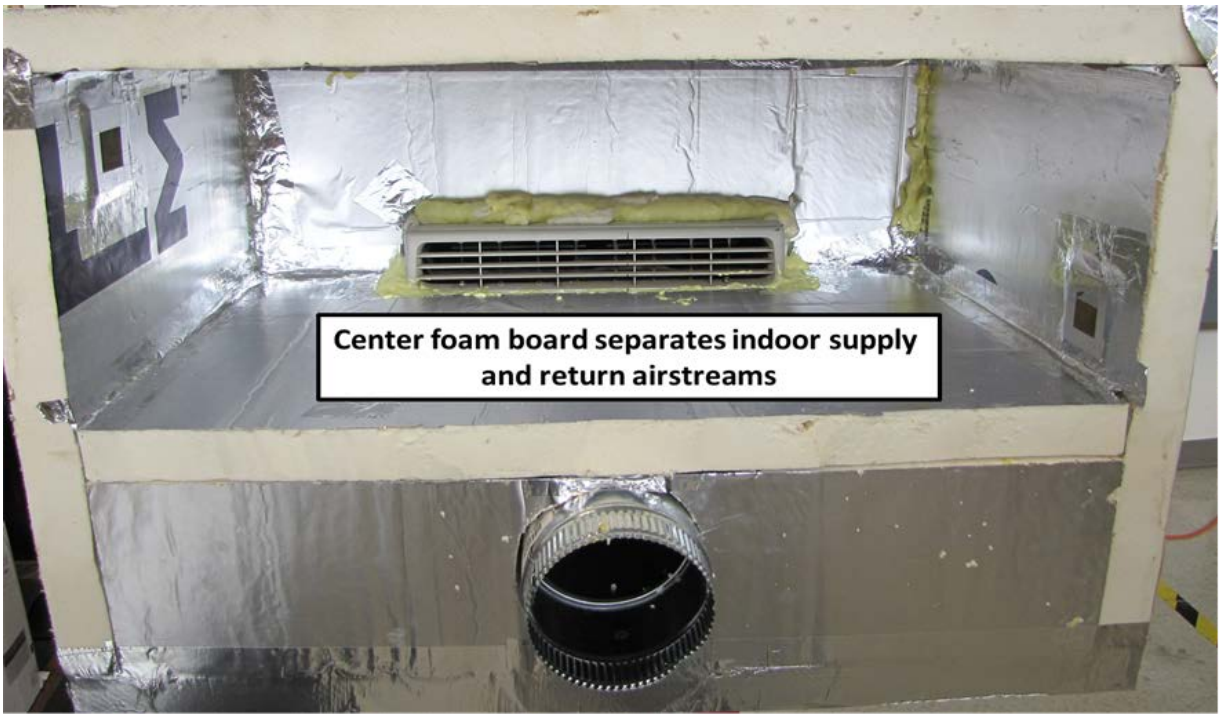

NREL/PIX 23664
Credit: Jeff Tomerlin, NREL

Figure 13. Further development of the plenum bisects the chamber, separating supply and return

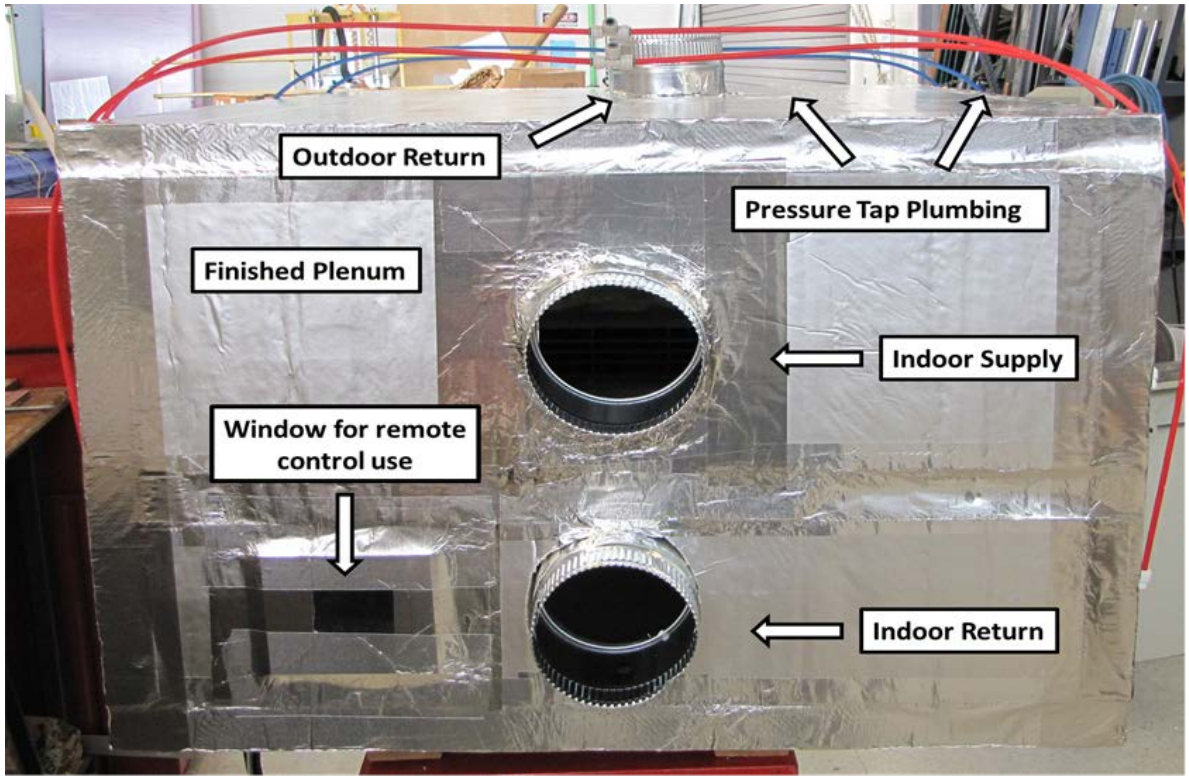

NREL/PIX 23665
Credit: Jeff Tomerlin, NREL

Figure 14. Completed plenum, completely sealed inside and out using foil tape. Six-inch ducts were installed to interface with the HVAC laboratory.

4.1.2 Condensate Injection

All test units drain condensate from the evaporator side to the condenser side, and the condensate drips over the outside of the case after reaching the necessary water level. Two test units use a special ring around the condenser fan (Figure 15) that picks up the condensate as it flows toward the condenser and sprays it onto the condenser for additional cooling.

NREL/PIX 23666
Credit: Jeff Tomerlin, NREL

Figure 15. The condensate pick-up ring around the condenser fan

During our test this natural flow of condensate was blocked to measure it with a coriolis meter. To restore this spraying effect, we plumbed the condensate after the meter to an open reservoir, from which a peristaltic pump injected it directly back to the original drain outlet from the evaporator (Figure 16). This allowed the condensate to flow in its native fashion to the condenser fan ring for pickup (Figure 17). Lastly, an overflow pan and drain on the outside of the condenser was necessary in the event that humid conditions would cause the condensate to overflow the unit into the plenum. The drain kept condensate from collecting in the plenum and disrupting humidity measurements. A trap filled with water was installed in each drain's tubing to keep from losing air mass in that airstream.

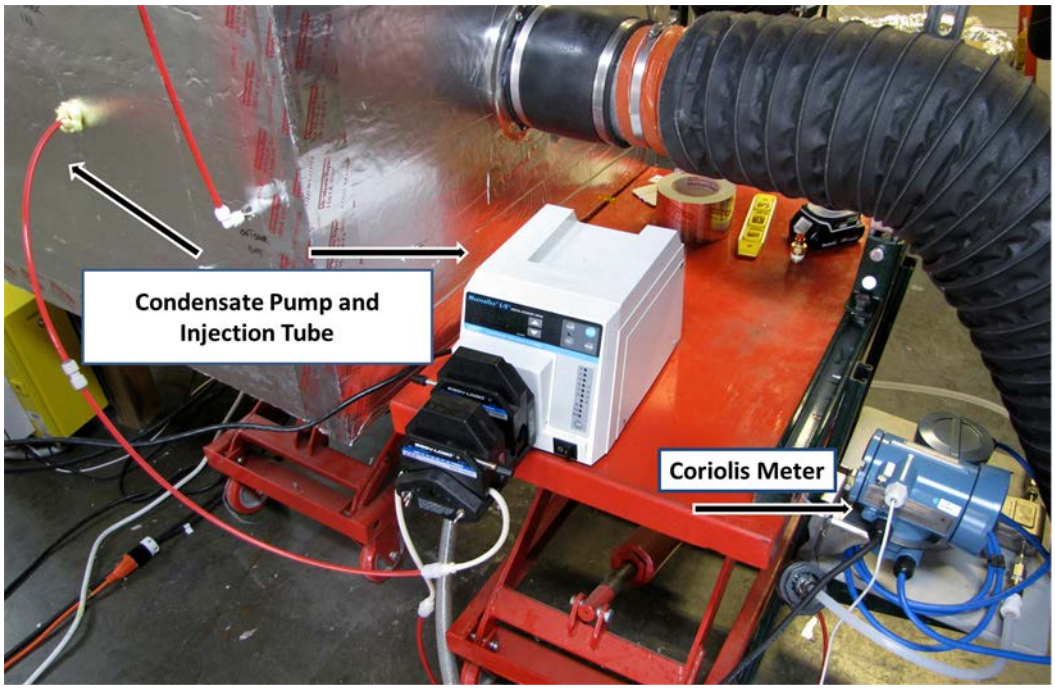

NREL/PIX 23667
Credit: Jeff Tomerlin, NREL

Figure 16. Peristaltic pump and condensate injection tube

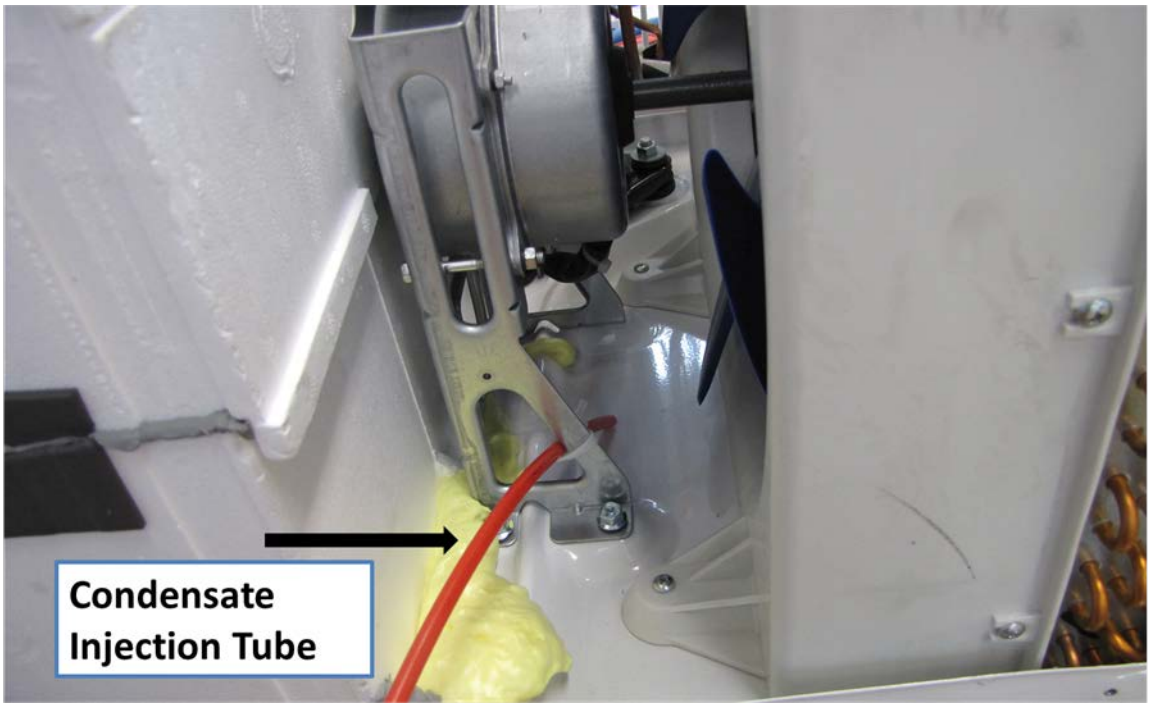

NREL/PIX 23662
Credit: Jeff Tomerlin, NREL

Figure 17. Condensate injection tube location just downstream of evaporator drain

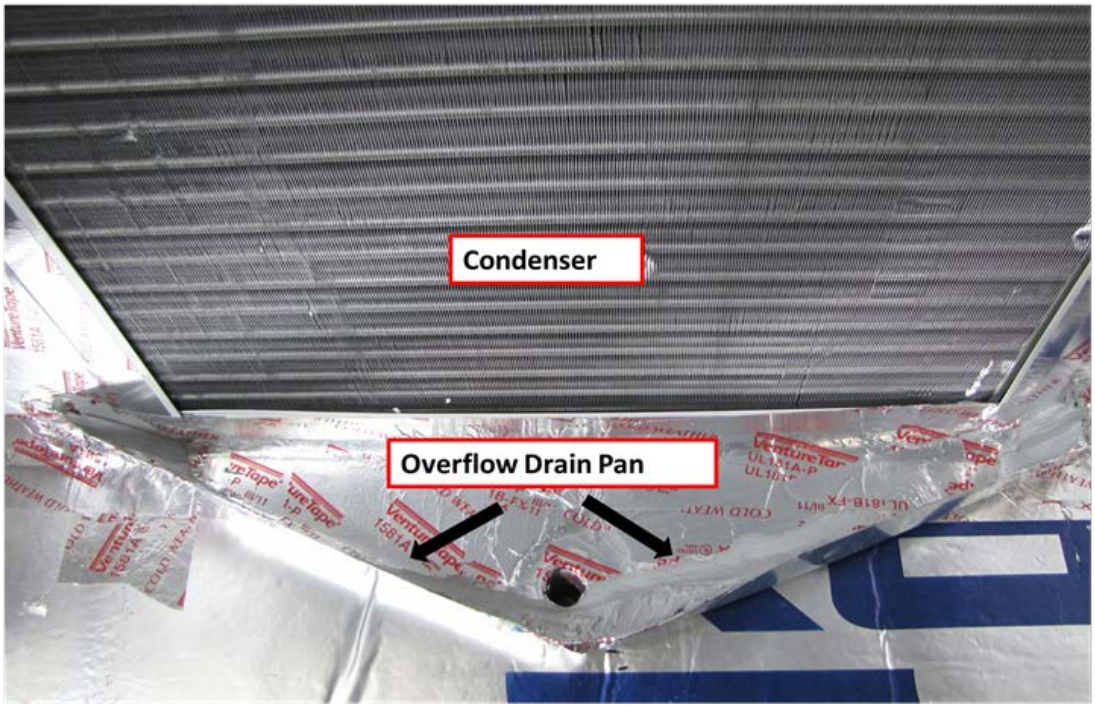

NREL/PIX 23669
Credit: Jeff Tomerlin, NREL

Figure 18. The condenser overflow pan and drain

4.2 Test Conditions

ASHRAE Standard 16 requires a windows AC to be tested at only a single operating point (ASHRAE 2009), and most manufacturers report the performance at this operating point only. The rated operating point is an evaporator return condition of 80°F (26.7°C) dry-bulb (DB) and 67°F (19.4°C) wet-bulb (WB) and a condenser inlet temperature of 95°F (35°C). Performance at a single operating point does not provide adequate information to develop accurate performance models for all operating conditions (Cutler et al. 2013). Therefore, during the current study, each window AC was tested at four evaporator return conditions and five condenser inlet temperatures resulting in a total of 20 steady-state operating points.

The four return air test conditions are shown on the psychrometric chart in Figure 19 and listed in Table 4. The condenser inlet temperatures are also shown in Figure 19 and listed in Table 5. We verified that the outdoor humidity did not have a significant impact on the window AC performance (see Section 4.3); thus, the outdoor humidity was held constant during the tests.

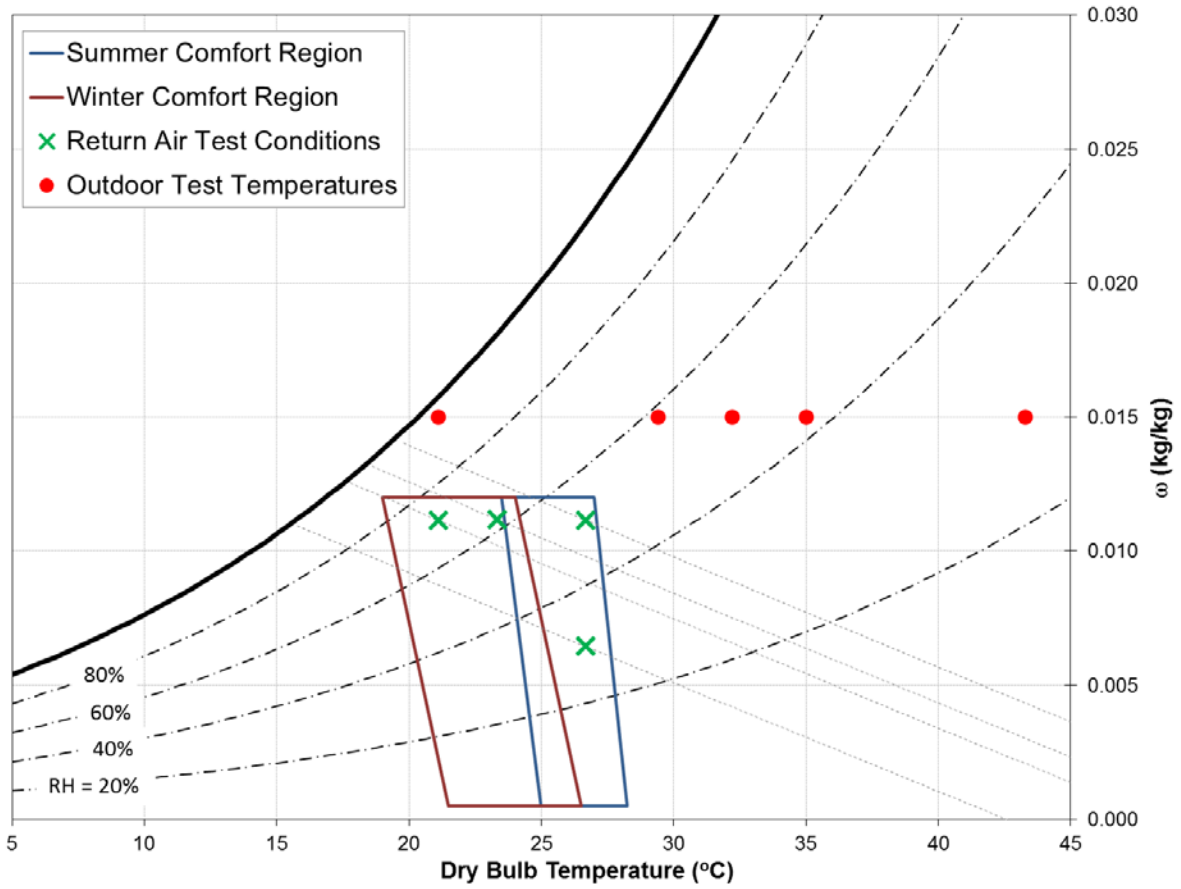

Figure 19. Psychrometric chart showing air conditioner test points in winter and summer comfort regions from ASHRAE (2004)

Table 4. Indoor Return Air Test Conditions

Indoor Return Test Point	DB		WB		DP		Relative Humidity (%)
	(°C)	(°F)	(°C)	(°F)	(°C)	(°F)	
1	26.7	80	19.4	67	15.8	60.4	51.1
2	23.3	74	18.4	65.1	15.8	60.4	62.5
3	21.1	70	17.6	63.7	15.7	60.3	71.3
4	26.7	80	---[1]	---[1]	---[1]	---[1]	---[1]

[1] Humidity was low enough to ensure dry coil operation

Table 5. Outdoor DB Temperature Test Points

Outdoor Test Point	DB	
	(°C)	(°F)
1	21.1	70
2	29.4	85
3	32.2	90
4	35.0	95
5	43.3	110

4.3 Steady-State Test Results

As mentioned in Section 3, the percent of flow recirculated from the evaporator supply to return was quite high. A psychrometric-based model was developed to account for the recirculation and all results presented in this report have used this model to account for the recirculation. The capacity and COP were degraded by up to 15% at several test points but, under most operating conditions, was around 5%–10%.

4.3.1 Measured and Manufacturer Report Performance Comparison

Table 6 compares the measured performance to manufacturer-reported values at the standard operating point. Low, medium, and high fan speeds are included, because manufacturers do not report the fan setting that coincide with the reported performance values. Because manufacturers report performance only at the standard rating point, a direct comparison to manufacturer-provided data can be conducted only at this specific point of operation.

Table 6. Comparison of Rated and Measured Performance

Window AC	Manufacturer Rated Performance[1]		Measured Performance Estimates[1]	
	Capacity (Btu/h)	EER (Btu/Wh)	Capacity[2] (Btu/h)	EER[2] (Btu/Wh)
Frigidaire (FRA103BT1)	10,000	9.8	9,117 ± 390 9,298 ± 424 9,547 ± 473	8.8 ± 0.4 8.9 ± 0.4 8.9 ± 0.4
Frigidaire (FRA106CV1)	10,000	10.7	10,001 ± 440 10,028 ± 447 10,256 ± 529	11.5 ± 0.5 11.5 ± 0.6 11.0 ± 0.5
Haier	5,000	9.7	4,514 ± 195 4,767 ± 194 4,937 ± 213	8.2 ± 0.3 8.8 ± 0.4 9.0 ± 0.4
GE (AGD06LAG1)	6,000	9.7	3,497 ± 222[3]	4.3 ± 0.3[3]

[1] Performance at the rated return condition of 80°F (26.7°C) DB, 67°F (19.4°C) WB, and outdoor condition of 95°F (35°C). NREL is not a certified test laboratory.
[2] Values are for low, medium, and high fan speeds, respectively.
[3] All tests were conducted using the medium fan speed because there was little variation between measured low, medium, and high airflow rates.

Complete experimental datasets are included in Appendix B.

4.4 Steady State Performance Maps

Performance maps allow the performance at any operating point (within the numerical bounds of the map) to be estimated. Performance maps were developed using the experimental datasets (located in Appendix B) based on the AC modeling algorithms included in the EnergyPlus simulation engine (DOE 2010). Biquadratic equations are commonly used to simulate HVAC equipment, and measured data are fit to the curves through least-squares regression.

4.4.1 Performance Map Coefficients

EnergyPlus predicts off-rated performance by scaling the rated performance values (listed in Table 6) by two multipliers – one to account for varying operating temperatures and one for flow rate. Off-rated performance is estimated using Equations 7 and 8, which use the curve-fits in Equations 9 and 10, where T_{ewb} is the evaporator entering wet-bulb, T_{out} is the outdoor DB, and ff is the air flow fraction $\left(\dot{V}/\dot{V}_{rated}\right)$. The energy input ratio (EIR) is the inverse of the COP. The apparatus DP model is used to predict the operating sensible heat ratio (SHR). (DOE 2010)

$$\dot{Q}_{tot} = \dot{Q}_{tot,rated} \cdot f_{T,\dot{Q}} \cdot f_{ff,\dot{Q}} \tag{7}$$

$$EIR_{tot} = EIR_{rated} \cdot f_{T,EIR} \cdot f_{ff,EIR} \tag{8}$$

$$\left(f_{T,\dot{Q}}, f_{T,EIR}\right) = a + b \cdot T_{ewb} + c \cdot T_{ewb}^2 + d \cdot T_{out} + e \cdot T_{out}^2 + f \cdot T_{ewb} \cdot T_{out} \tag{9}$$

$$\left(f_{ff,\dot{Q}}, f_{ff,EIR}\right) = a + b \cdot ff + c \cdot ff^2 \tag{10}$$

Temperature-based performance curve coefficients are listed in Table 7 and Table 8 and were generated using the medium fan speed as the rated airflow rate.

Table 7. Temperature (°C) Performance Curve Coefficients for the Frigidaire FRA103BT1 and Frigidaire FRA106CV1 Window ACs

	Frigidaire (FRA103BT1)	
	Total Capacity Multiplier $\left(f_{T,\dot{Q}}\right)$	EIR Multiplier $\left(f_{T,EIR}\right)$
a	8.477E-1	5.111E-1
b	7.225E-3	1.505E-2
c	8.902E-4	–4.509E-4
d	2.077E-3	7.401E-3
e	–9.272E-5	3.901E-4
f	–4.148E-4	–5.426E-4
r^2	0.999	0.999

	Frigidaire (FRA106CV1)	
	Total Capacity Multiplier $\left(f_{T,\dot{Q}}\right)$	EIR Multiplier $\left(f_{T,EIR}\right)$
a	6.405E-1	2.287
b	1.568E-2	–1.732E-1
c	4.531E-4	4.745E-3
d	1.615E-3	1.662E-2
e	–1.825E-4	4.840E-4
f	6.614E-5	–1.306E-3
r^2	0.993	0.994

Table 8. Temperature (°C) Performance Curve Coefficients for the Haier HWR-5XCL and GE AGD06LAG1 Window ACs

	Haier (HWR-5XCL)		GE (AGD06LAG1)	
	Total Capacity Multiplier $\left(f_{T,\dot{Q}}\right)$	EIR Multiplier $\left(f_{T,EIR}\right)$	Total Capacity Multiplier $\left(f_{T,\dot{Q}}\right)$	EIR Multiplier $\left(f_{T,EIR}\right)$
a	1.491	–3.271E-2	–3.398	2.603E-1
b	–8.451E-2	5.632E-2	4.175E-1	4.857E-2
c	3.559E-3	–9.628E-4	–8.737E-3	–1.507E-3
d	–6.417E-4	3.708E-2	9.807E-3	–6.034E-3
e	–1.918E-4	4.817E-4	–2.138E-4	6.581E-4
f	1.197E-4	–2.405E-3	–7.402E-4	–3.196E-4
r^2	0.934	0.930	0.999	0.999

Flow fraction-based performance curves are listed in Table 9 and Table 10 and were generated at the rated operating condition of 80°F (26.7°C) return DB, 67°F (19.4°C) return WB, and 95°F (35°C) outdoor DB temperatures. The GE unit was not tested at different airflow rates because the measured flow rates for the three fan speeds were quite similar. Thus, flow fraction curves for the GE unit could not be generated. The performance as a function of flow rate was nearly linear, thus *c* in Equation 10 was set to 0. However, the behavior of Frigidaire FRA106CV1 was not similar to the other two units and a linear fit did not work well for the EIR performance curve.

Table 9. Flow Fraction Performance Curve Coefficients for the Frigidaire FRA103BT1 and Frigidaire FRA106CV1 Window ACs

	Frigidaire (FRA103BT1)		Frigidaire (FRA106CV1)	
	Total Capacity Multiplier $\left(f_{ff,\dot{Q}}\right)$	EIR Multiplier $\left(f_{ff,EIR}\right)$	Total Capacity Multiplier $\left(f_{ff,\dot{Q}}\right)$	EIR Multiplier $\left(f_{ff,EIR}\right)$
a	7.957E-1	1.092	8.870E-1	1.763
b	2.053E-1	–8.983E-1	1.128E-1	–6.081E-1
r^2	0.999	0.952	1.0	0.206

Table 10. Flow Fraction Performance Curve Coefficients for the Haier HWR-5XCL Window AC

	Haier (HWR-5XCL)	
	Total Capacity Multiplier $\left(f_{ff,\dot{Q}}\right)$	EIR Multiplier $\left(f_{ff,EIR}\right)$
a	4.416E-1	1.623
b	5.484E-1	–6.044E-1
r^2	0.962	0898

4.4.2 Window AC Performance Curves Compared to Single-Speed Split Systems

Figure 20 and Figure 21 display the temperature-based performance curves for the Frigidaire FRA106CV1 as a function of outdoor DB (condenser inlet) and evaporator entering wet-bulb (EWB) temperatures. Additional performance curve plots are included in Appendix C.

Normalized COP (as opposed to EIR) is included in the plots to help visualize the AC's performance. The normalized total capacity and COP are equal 1 at a 67°F (19.4°C) EWB temperature and 95°F (35°C) condenser inlet temperature. Both curves exhibit the expected behavior—both capacity and COP decrease with increasing outdoor DB and decreasing evaporator EWB. Air conditioners are most efficient at low outdoor and high EWB temperatures because this minimizes the temperature lift at which the unit must pump heat across.

Figure 22 and Figure 23 compare the temperature-based performance curves for the Frigidaire FRA106CV1 window AC (solid lines) to a typical single-speed split system (dashed lines). The curves for the single-speed split system were taken from Cutler et al. (2013). Capacity and COP curves behave similarly to the split system curves; however, the capacity and COP are more adversely affected by a lower entering WB temperature. The performance at high outdoor temperatures relative to the rated performance was better than initially expected for this unit. Figure 23 shows the COP of this particular window AC degrades less at higher outdoor temperatures than does the typical single-speed split system presented by Cutler et al. (2013).

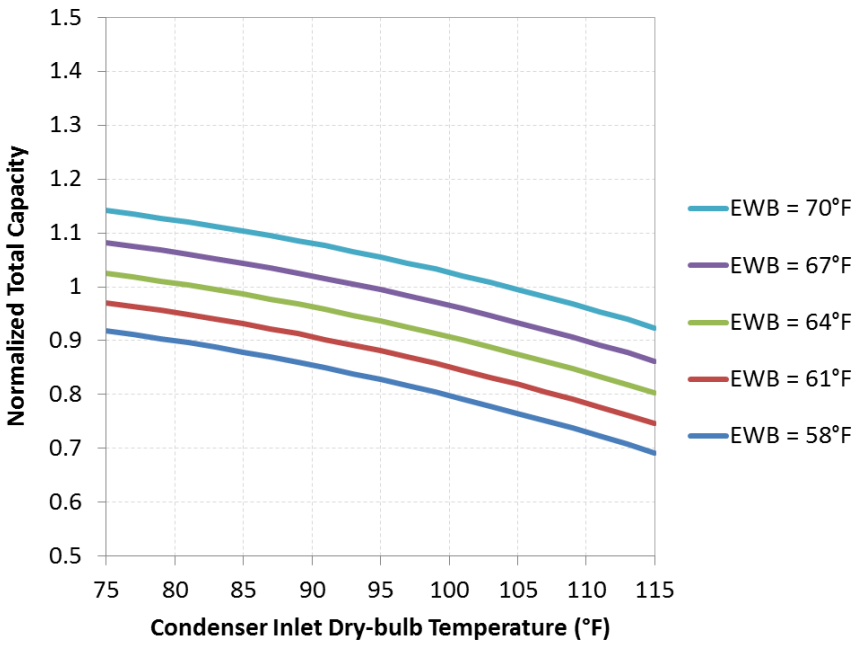

Figure 20. Total capacity temperature-based performance curves for the Frigidaire FRA106CV1

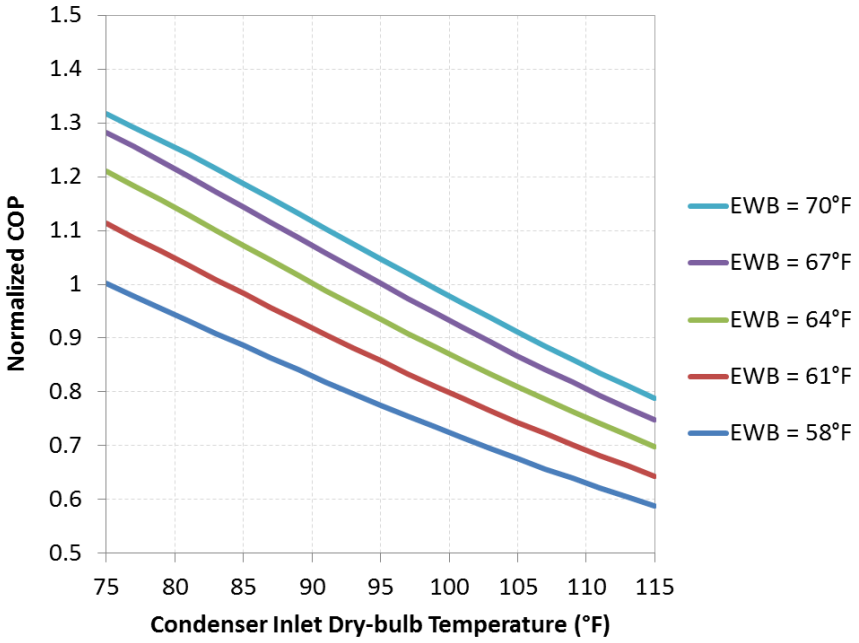

Figure 21. COP (1/EIR) temperature-based performance curves for the Frigidaire FRA106CV1

Figure 24 shows the normalized total capacity and COP (1/EIR) flow fraction performances for the Haier window AC. Additional flow fraction performance curve plots are included in Appendix D.

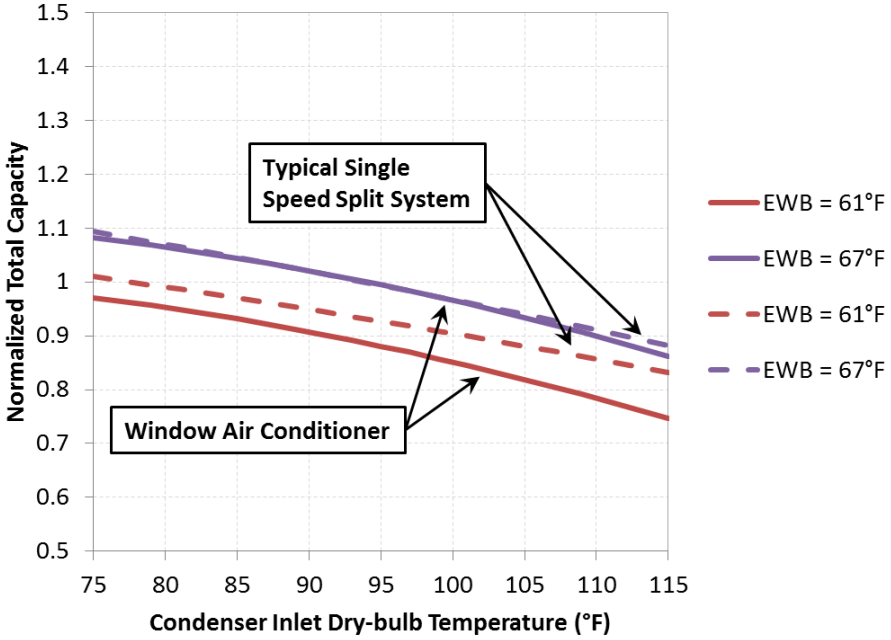

Figure 22. Comparing total capacity performance curves for the Frigidaire FRA106CV1 (solid lines) to a typical single-speed split system (dashed lines)

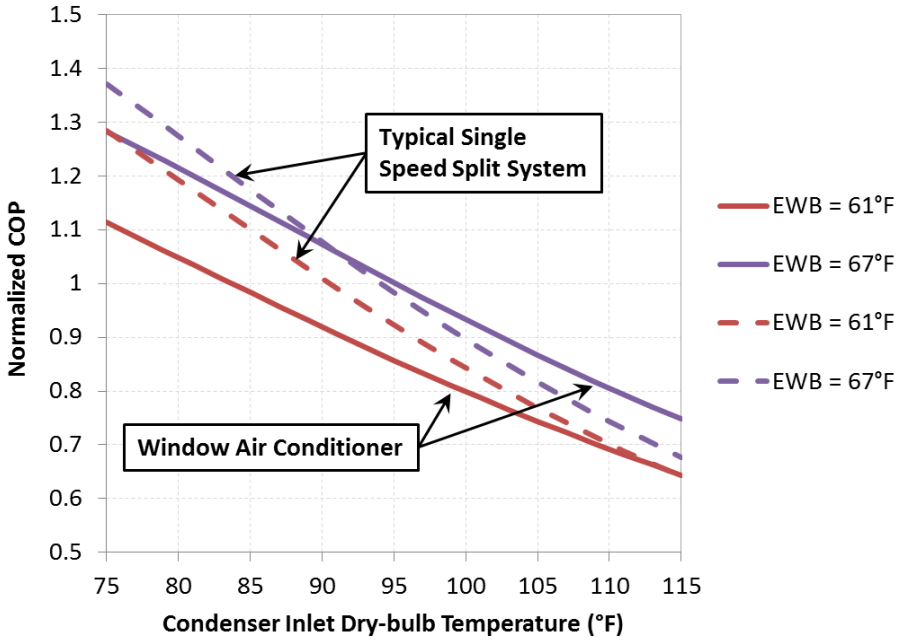

Figure 23. Comparing COP performance curves for the Frigidaire FRA106CV1 (solid lines) to a typical single-speed split system (dashed lines)

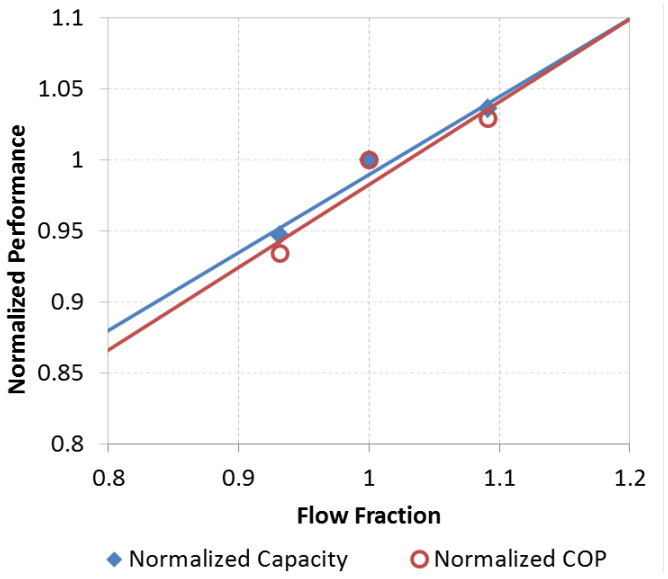

Figure 24. Capacity and COP flow fraction performance curves for the Haier HWR-5XCL

Figure 25 compares the flow fraction performance curves for the Haier window AC (solid lines) to a typical single-speed split residential system from Cutler et al. (2013) (dashed lines). Total capacity and COP have a similar trend (albeit different slopes) between the two types of units—capacity and COP decrease as the airflow rate across the coil decreases. A window AC uses a

single motor shaft to power the evaporator and condenser fans, so the window AC will be more affected by changing the fan speed than split systems because both the evaporator and condenser airflow rates are affected. This explains the steeper slope compared to a typical split system.

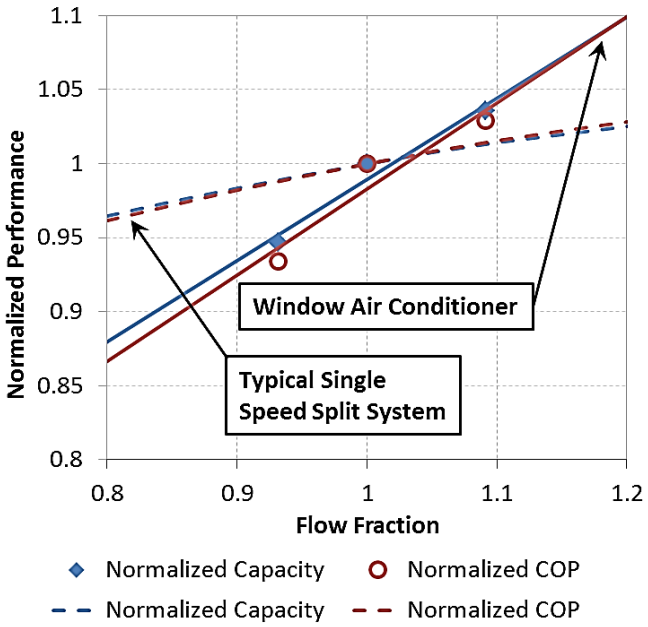

Figure 25. Comparing flow fraction performance curves for the Haier HWR-5XCL (solid lines) to a typical single-speed split system (dashed lines)

4.5 Cyclic Test Results

All four units tested included a built-in thermostat to enable room temperature control by cycling the compressor. Thus, cyclic performance degradation must be experimentally determined to enable an accurate calculation of window AC energy use. ASHRAE Standard 16-1983 does not include a test procedure to determine the cyclic performance of window ACs, because the test apparatus prescribed by the standard not does support such a test (ASHRAE 2009).

The cyclic degradation coefficient (C_D) quantifies a unit's ability to efficiently reach steady state and was experimentally determined for each unit by following AHRI Standard 210/240 test procedures (ANSI/AHRI 2008). After completing the steady-state dry-coil C-Test (80°F [26.7°] return DB, 82°F [27.8°C] outdoor temperature), the unit's compressor was cycled off for 24 min and then on for 6 min ($\Delta\tau_{cyc,dry}$ = 0.5 h). Data from the third on/off cycle were used to calculate C_D using Equations 11 through 16. The cooling load factor (CLF), calculated using Equation 15, is the ratio of total cooling capacity during a single on-off period to the steady-state capacity.

$$q_{cyc,dry} = \int_{\tau_1}^{\tau_2} \left[\frac{\dot{m}_{evap,in}(\tau) + \dot{m}_{evap,out}(\tau)}{2} \right] \left[h_{evap,in}(\tau) - h_{evap,out}(\tau) \right] d\tau \quad (11)$$

$$e_{cyc,dry} = \int_{\tau_1}^{\tau_2} \dot{P}(\tau) d\tau \quad (12)$$

$$EER_{cyc,dry} = \frac{q_{cyc,dry}}{e_{cyc,dry}} \quad (13)$$

$$EER_{ss,dry} = \frac{\dot{Q}_{ss,dry}}{\dot{P}_{ss,dry}} \quad (14)$$

$$CLF = \frac{q_{cyc,dry}}{\dot{Q}_{ss,dry} \cdot \Delta\tau_{cyc,dry}} \quad (15)$$

$$C_D = \frac{1 - \frac{EER_{cyc,dry}}{EER_{ss,dry}}}{1 - CLF} \quad (16)$$

C_D values are included in Table 11. $EER_{ss,dry}$ values correspond the AHRI steady-state, dry-coil C-Test condition of 80°F (26.7°) return DB, 82°F (27.8°C) outdoor temperature. $EER_{cyc,dry}$ tests were run at the same operating condition and all cyclic tests were conducted at the medium fan speed.

Table 11. Window AC Measured Cyclic Degradation

Window AC	$EER_{cyc,dry}$ [1] (Btu/Wh)	$EER_{ss,dry}$ [2] (Btu/Wh)	CLF	C_D [3]
Frigidaire (FRA103BT1)	8.04	9.75	0.20	0.22
Frigidaire (FRA106CV1)	8.07	9.92	0.15	0.22
Haier	6.88	8.23	0.16	0.20
GE (old)	3.02	5.51	0.13	0.52

[1] Corresponds to AHRI Standard 210/240 D-Test (ANSI/AHRI 2008)
[2] Corresponds to AHRI Standard 210/240 C-Test (ANSI/AHRI 2008)
[3] A maximum C_D of 0.25 is used in SEER calculations (ANSI/AHRI 2008)

Figure 26 shows the transient cyclic test for the Frigidaire FRA106CV1. The cyclic tests for the other three window ACs were similar. Data from the third cycling period were used to calculate the values in Table 11.

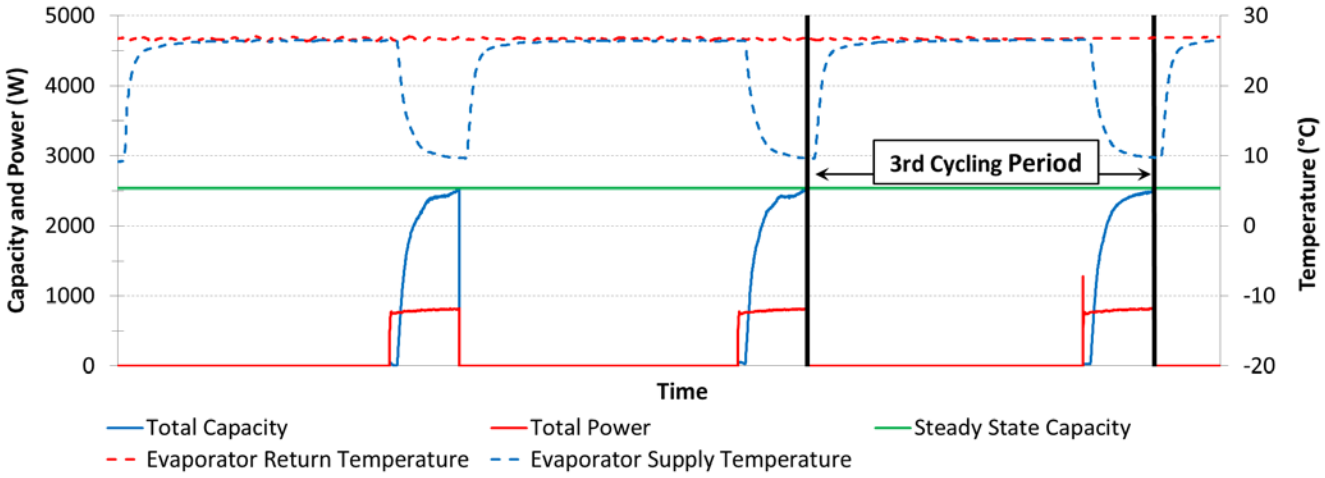

Figure 26. Time-series plot showing cyclic testing

4.6 Equivalent Seasonal Energy Efficiency Ratio

SEER is the industry rating figure of merit for unitary split air conditioners, prescribed by AHRI Standard 210/240. Although not defined by ASHRAE Standard 16, our test method enabled calculation of an equivalent SEER to estimate of the average seasonal efficiency and allows the performance of the tested window ACs to be more easily compared to residential split ACs. The cyclic testing (described in Section 4.4) allowed the SEER for the window ACs to be estimated.

For single-speed systems, SEER is calculated using

$$SEER = \left(1 - 0.5 \cdot C_D\right) \cdot EER_B \tag{17}$$

where C_D was taken from Table 11 and EER_B was determined using the performance curves (presented in Section 4.3) evaluated at T_{ewb} = 67°F (19.4°C) and T_{out} = 82°F (27.8°C) (ANSI/AHRI 2008).

Table 12 contains the SEER values for the four window ACs tested. These values are for the unit only and do not account for added energy use caused by increased infiltration from the installation. Though SEER values are not useful in developing simulation models, they are useful when comparing AC products. SEER 13 is the minimum efficiency available on the market and high efficiency, variable-speed split systems can achieve SEER 24. Only the Frigidaire ENERGY STAR unit achieves a SEER approaching the minimum efficiency for split systems.

Table 12. Equivalent SEER for Window ACs

Window AC	Equivalent SEER[1] (Btu/Wh)
Frigidaire (FRA103BT1)	9.3
Frigidaire (FRA106CV1)	12.1
Haier	9.9
GE (old)	4.7

[1] Neglects air infiltration, but includes air recirculation. NREL is not a certified ratings laboratory, and these estimates are based on measured performance.

4.7 Performance Impact of Condensate Spray

As mentioned in Section 4.1, special measures had to be taken to account for the condenser fan's ability to spray collected condensate onto the condenser coil without sacrificing the condensate mass flow measurement. The impact of this feature was examined for the Haier unit by first running a test without re-injecting the condensate back into the unit and then testing the unit while injecting the condensate at varying outdoor WB temperatures.

The results of this test are plotted in Figure 27. The blue and red solid lines are measured total cooling capacity (left y-axis) and EER (right y-axis), respectively, when condensate injection was removed. The individual points represent the measured performance when the condensate was injected into the condenser side and was therefore sprayed onto the condenser coil. Error bars have been included based on an uncertainty analysis. The data in Figure 27 were collected at a 80°F (26.7°C) DB, 67°F (19.4°C) WB evaporator return condition, and 95°F (35°C) outdoor DB.

The results show that unit performance declines slightly with increasing outdoor WB temperature. However, the performance benefit of condensate spray was significant with an approximate 7% increase in the capacity and 14% increase in the EER (or COP). The performance at the lower WB temperatures may be slightly overestimated, because the unit is unlikely to generate much indoor condensate at low outdoor WB temperatures. Because of the small dependence on outdoor humidity, all other tests were run at a single outdoor DP temperature of approximately 60°F (15.5°C).

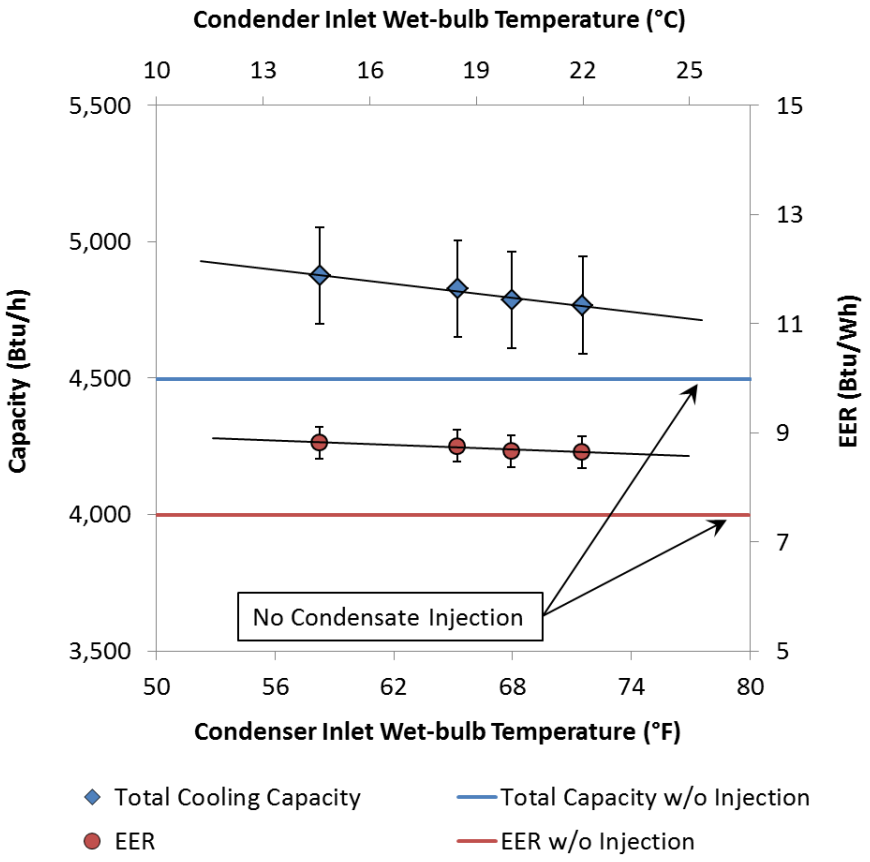

Figure 27. Performance impact of condenser fan condensate spray at different outdoor WB temperatures

5 Conclusions

This report describes detailed, system performance testing of four residential window AC units to enable whole-building integration analysis. All testing was conducted at NREL's Advanced HVAC Systems Laboratory. There were three major components to the testing. Air infiltration testing was performed on the units to characterize installation effects and internal leakage, supply air recirculation for the condenser and evaporator were measured, and the performance characteristics of each refrigeration system were measured under steady and cyclic operation, including the effects of condensate re-evaporation. These tests provide new insights into the installed performance of window AC units. This information is critical to accurate building simulation and energy savings predictions and provides insights into potential design improvements for future products.

The infiltration testing was performed using a pressurized plenum chamber with accurate, time resolved pressure and flow measurements. Air leakage through pathways internal to the case was fairly modest, roughly 1–2 cfm under normal operation. Infiltration resulting from installation in a window, following manufacturer instructions, was significant. The measured installation leakage was equivalent to a 27–42 $in.^2$ hole in the wall. This is not surprising when the affected sealing perimeter is measured and adds to more than 200 linear inches. It does motivate improvement in installation methods, both by manufacturers to provide better attachments and instructions, and for product owners to retrofit their ACs with a small amount of insulating foam board and some tape, at a cost of less than $15. Careful installation can reduce window AC leakage by 65%–85%, compared with following manufacturer installation instructions.

Recirculation testing was performed via a novel technique that used IR images and the correlation between thermal and mass distributions in the flow field to infer recirculation on the evaporator and condenser of each unit. This is a new and valuable technique for quantitative flow measurements due to the rapid nature of the experimental setup, high spatial and (if needed) temporal resolution, and low capital costs. The units' performance was significantly degraded by evaporator recirculation. For new units the capacity degradation ranged from 2.5% to 14% with an average of 7% degradation, and cooling COP degradation ranged from 2.2% to 19% with an average of 8%. For the old unit, capacity degradation was significantly higher at an average of 22%, and COP degradation at an average 11.6%. This highlights the importance of properly maintaining window ACs, and of proper design to reduce air recirculation in future products. The performance mapping tests revealed what rated efficiency and capacity could be achieved if recirculation were eliminated completely. This potential for performance improvement is not made evident by standard rating tests and is essential for designers and manufacturers if they are to improve their products.

Units were tested under a wide range of temperatures and humidity. Resulting performance maps were compared to minimum-efficiency split systems, and performance curves behave similarly. Model input coefficients were provided for direct use by building simulation engineers. We estimated that window ACs deliver operating efficiency equivalent to SEER 9-12 when new. Insufficient maintenance can cause substantial performance degradation, as evidenced by the old GE unit where exceedingly fouled coils resulted in performance equivalent to a SEER 4.7 split system.

Together these tests provide previously unavailable information about the performance of window AC units. This information is critical for developing more accurate building simulation models and determining energy use of these units in real-world applications. The techniques developed and the quantitative information provided may be valuable to manufacturers and designers who are interested in improving performance and decreasing the cost of this class of products.

We feel there are opportunities for manufacturers to do better (listed in Table 13). Installation accessories did not satisfactorily enable the unit to be installed and operated at rated efficiency. The accessories are not included in the rating metric, so very little cost and design appear to be applied to them. The result is a high degree of air infiltration and low insulating value for the accessories, which result in overall performance reductions. Improvements should also be made to reduce air recirculation, either by supplying air from the bottom instead of top of the interior face, or by providing a fin attachment to help separate those airstreams.

Table 13. Summary of Potential Low-Cost Window AC Performance Improvements

Recommended Design Modification	Method to Achieve	Potential Performance Improvement
Reduce Installation Infiltration	• Provide better installation attachments such as closed-cell foam weather stripping, removable tape, and similar.	Infiltration reduced by up to 47 sq. in., or up to 90 cfm50
Reduce Air Recirculation	• Invert the interior components so evaporator supply is at the bottom. • Supply an attachment fin to separate supply and return airflows.	At least 1 EER
Reduce the Barriers to Excellent Maintenance	• Provide better air filters. • Provide an air filter for the condenser. • Provide a cage or grille to limit damage to condenser fins. • Provide a means to clean the refrigerant coils using a vacuum.	Up to 4 EER
Increase Airflows	• Provide better fan blade design, including scalloped trailing edges.	At least 1 EER Lower noise

We believe the manufacturers can make all these improvements with minimal additional cost. We are developing a practical owner's guide to facilitate owner retrofit of existing installed window ACs.

Knowing the performance parameters listed above, our next steps will be to evaluate existing building energy models to ensure they can accurately simulate window ACs. We present the results of our tests in a form that can be easily used in tools such as EnergyPlus. However, we have yet to validate the ZoneHVAC:WindowAirConditioner model and to demonstrate that it effectively models all significant phenomena we measured. That is left as future work.

References

ANSI/AHRI. (2008). Performance Rating of Unitary Air Conditioning and Air Source Heat Pump Equipment. ANSI/AHRI Standard 210/240. Arlington, VA: Air Conditioning, Heating, and Refrigeration Institute.

ASHRAE. (2004). Thermal Environmental Conditions for Human Occupancy. ASHRAE Standard 55-2004. Atlanta, GA: ASHRAE.

ASHRAE. (2009). Method of Testing for Rating Room Air Conditioners and Packaged Terminal Air Conditioners. ASHRAE Standard 16-1983 (RA 2009). Atlanta, GA: ASHRAE.

Booten, C.; Tomerlin, J.; Winkler, J. (expected for fall 2013). *Infrared Imaging Technique for Measuring Flow Mixing*. Golden, CO: National Renewable Energy Laboratory.

Booten, C. (2006). *Rapid Heat Transfer Measurements in Complex Internal Flows* Ph.D. thesis, Stanford University.

BSRIA. (2012). Packaged, Unitary and Furnaces Air Conditioning Windows & Moveables USA. Report 55301/22.

Cutler, D.; Winkler, J.; Kruis, N.; Christensen, C.; Brandemuehl, M. (2013). *Improved Modeling of Residential Air Conditioners and Heat Pumps for Energy Calculations*. NREL/TP-5500-56354. Golden, CO: National Renewable Energy Laboratory.

DOE. (2008). Packaged Terminal Air Conditioners and Heat Pumps Energy Conservation Standard Notice of Proposed Rulemaking Technical Support Document, Chapter 3, available at http://www1.eere.energy.gov/buildings/appliance_standards/commercial/pdfs/ptac_pthp_tsd/chapter_3.pdf. Accessed October 22, 2012.

DOE. (2010). EnergyPlus Engineering Reference. Washington, DC: U.S. Department of Energy.

DOE. (2013). Code of Federal Regulations, Title 10 – Energy, Part 431. Washington, DC: U.S. Department of Energy.

EPA (2011). ENERGY STAR Market & Industry Scoping Report: Packaged Terminal Air Conditioners and Heat Pumps, December 2011, at http://www.energystar.gov/ia/products/downloads/ESTAR_PTAC_and_PTHP_Scoping_Report_Final_Dec_2011.pdf. Accessed October 22, 2012

Incropera, F. and DeWitt, D. (2002). *Fundamentals of Heat and Mass Transfer* New York, NY, Wiley 5th Ed.

Mills, A.F. (1995). *Heat and Mass Transfer* Chicago, IL, Irwin.

Touloukian, Y.; DeWitt, D.; Hernicz, R. (1972). *Thermophysical Properties of Matter Volume 9 of TPRC Series* New York, NY, IFI/Plenum.

Appendix A: Description of End-of-Life Test Unit

We participated in a residential retrofit project in New Braunfels, Texas (hot-humid climate). The approximately 800-ft^2 house was cooled by three window ACs, two similar 6,000 Btu/h 9.7-EER GE units and a 5,400 Btu/h 10-EER unit branded Admiral. Throughout the spring, summer, and fall, these three units seldom cycled and struggled to deliver sufficient cooling for the poorly insulated structure. The homeowners were disappointed by the noisy ACs that did not maintain thermal comfort, and decided to change out one window AC with a new, higher capacity, higher efficiency unit. (The home was planned for a scrape-and-rebuild, so insulation and similar measures were not considered. The homeowners were counseled on the benefits of air sealing, which may still be cost effective for the short remaining life of the home.)

A 10,000 Btu/h 10.2-EER LG unit was purchased and installed in place of one of the GE units. The retired unit was returned to NREL for end-of-life testing.

During the retrofit, we noted many opportunities for energy and performance improvements in the window ACs' installations. These are fairly typical from our installation experience to date.

Installation issue #1: Manufacturer-provided attachments do not seal around the unit. Figure 28 shows one of the eight obvious air leak paths between the accordion wing attachments and the window frame.

NREL/PIX 23647 (left), 23646 (right)
Credit: Dane Christensen, NREL

Figure 28. Window AC before retrofit (right). Left view shows a portion of the area where installation air sealing was unsuccessful. The cobwebs, moisture damage, and dirt are further indications of long-term airflow.

Manufacturer-provided means to seal between the window sashes are also insufficient. Window ACs are often accompanied by a foam strip with instructions to install between the window panes to seal out airflow. As shown in Figure 29, when the foam is well installed between window panes it does not completely block air, but instead acts as an air filter and collects grime between the panes of glass. Moreover, these foam pieces are challenging to cut appropriately and

to install correctly to maximize their small benefit. They often slip down between window panes and fail to deliver the expected benefit.

NREL/PIX 23648 (left), 23649 (right), 23650 (top)
Credit: Dane Christensen, NREL

Figure 29. Window AC from the home's exterior (top). Bottom left image shows the window above the tested unit, with foam strip in place between window panes to block airflow. The foam acted as an air filter and did not block air, as indicated by the roughly 12 months of buildup between the otherwise clean window panes. Bottom right image shows the window above the other GE window AC, with the same foam strip installed incorrectly and failing to filter or block appreciable airflow.

Installation issue #2: Manufacturer-provided means to direct condensate outside the building are often ineffective. The end-of-life unit tested was draining all condensate back into the home, effectively reducing unit capacity and performance, increasing indoor humidity, and contributing to building decay. Figure 30 shows moisture damage around a wall AC installed in a different building, which we believe was caused by condensate leakage as well as infiltration humidity.

NREL/PIX 23651
Credit: Dane Christensen, NREL

Figure 30. Wall AC showing infiltration- and condensate-caused water damage to interior paneling

Installation issue #3: Failure to maintain the unit. AC coils are typically protected by well-designed air filters that provide decent protection from coil fouling when changed regularly. Our surveys showed nearly universal fouling of heat exchangers, louvers, and grilles. Manufacturer-provided air filters appear to be insufficient to filter the air, air infiltration in the case introduce significant fouling media, and homeowners are not diligent about cleaning the appliances or are uninformed of the impact that fouling has on performance. Fouling on the indoor grilles and heat exchangers may also contribute to health issues such as asthma and allergies, by retaining moisture and providing food for mold growth. Fouling is worse on the exterior coils, as there is no air filter. There, it blocks airflow and can significantly reduce airflow through the condenser. This problem is exacerbated relative to split systems because the heat exchanger is more compact and thus more difficult to clean. Figure 31 and Figure 32 show the fouled heat exchangers from our legacy test unit.

NREL/PIX 23652
Credit: Jeff Tomerlin, NREL

Figure 31. Fouling on the evaporator coil of a window AC

NREL/PIX 23653
Credit: Jeff Tomerlin, NREL

Figure 32. Fouling on the condenser coil of a window AC

Significant air infiltration also occurred through some units' cases. These leakage pathways are fully in the manufacturers' control, and cost considerations likely result in inadequate air sealing between the indoor and outdoor sections of the unit. Figure 33 shows one such example.

NREL/PIX 23654
Credit: Dane Christensen, NREL

Figure 33. Daylight shining through a window AC firewall. We were unable to locate a fresh air damper, which is a feature of some window ACs and may have provided the opening for this light, which indicates the presence of a large hole, and thus air infiltration.

Appendix B: Summary of Measured and Calculated Test Data

Table 14. Steady-State Experimental Test Data for the Frigidaire FRA103BT1

Return DB		Return WB		Return DP		Outdoor DB		Fan Speed	Total Capacity		SHR	Total Power	COP	EER (Btu/Wh)	Balances				
(°C)	(°F)	(°C)	(°F)	(°C)	(°F)	(°C)	(°F)		(W)	(Btu/h)		(W)			$\varepsilon_{M,evap}$	$\varepsilon_{M,cond}$	$\varepsilon_{M,total}$	ε_{E}	ε_{W}
26.7	80.0	19.6	67.3	16.0	60.8	21.0	69.9	894.5	3,161 ±126	10,785 ±431	0.61 ±0.01	895	3.5 ±0.1	12.1 ±0.5	1.00	1.04	1.02	1.02	1.01
26.7	80.1	19.6	67.3	16.0	60.9	29.4	84.9	986.4	2,932 ±125	10,004 ±427	0.62 ±0.01	986	3.0 ±0.1	10.1 ±0.4	1.00	1.04	1.03	1.03	1.01
26.7	80.0	19.4	67.0	15.7	60.3	32.2	90.0	1018.0	2,822 ±125	9,629 ±425	0.63 ±0.01	1,018	2.8 ±0.1	9.5 ±0.4	1.00	1.04	1.03	1.03	1.01
26.7	80.0	19.7	67.5	16.3	61.3	35.1	95.1	1041.0	2,672 ±114	9,117 ±390	0.61 ±0.01	1,041	2.6 ±0.1	8.8 ±0.4	0.99	1.04	1.02	1.03	1.01
26.7	80.0	19.4	66.9	15.6	60.1	35.0	95.0	1048.0	2,725 ±124	9,298 ±424	0.64 ±0.01	1,048	2.6 ±0.1	8.9 ±0.4	1.00	1.04	1.03	1.04	1.02
26.8	80.2	19.6	67.2	15.9	60.6	35.1	95.1	1068.0	2,798 ±139	9,547 ±473	0.65 ±0.01	1,068	2.6 ±0.1	8.9 ±0.4	0.99	1.04	1.02	1.03	1.00
26.7	80.1	19.3	66.7	15.5	59.8	43.3	110.0	1148.0	2,427 ±123	8,281 ±421	0.67 ±0.02	1,148	2.1 ±0.1	7.2 ±0.4	1.00	1.04	1.03	1.04	1.01
23.3	73.9	18.5	65.3	16.0	60.7	22.4	72.4	900.5	3,040 ±125	10,372 ±425	0.55 ±0.01	901	3.4 ±0.1	11.5 ±0.5	1.00	1.03	1.02	1.02	1.01
23.3	73.9	18.5	65.3	16.0	60.8	29.4	85.0	976.9	2,852 ±123	9,731 ±421	0.55 ±0.01	977	2.9 ±0.1	10.0 ±0.4	1.00	1.03	1.02	1.03	1.02
23.3	73.9	18.6	65.5	16.2	61.1	32.3	90.1	1012.0	2,755 ±123	9,400 ±420	0.55 ±0.01	1,012	2.7 ±0.1	9.3 ±0.4	1.00	1.04	1.02	1.03	1.01
23.3	73.9	18.7	65.6	16.3	61.3	35.0	95.0	1045.0	2,667 ±123	9,100 ±420	0.55 ±0.01	1,045	2.6 ±0.1	8.7 ±0.4	1.00	1.04	1.02	1.03	1.01
23.3	73.9	18.5	65.2	15.9	60.6	43.3	110.0	1140.0	2,368 ±122	8,080 ±418	0.57 ±0.01	1,140	2.1 ±0.1	7.1 ±0.4	1.00	1.04	1.03	1.04	1.02
21.8	71.2	18.1	64.6	16.1	61.0	21.8	71.3	894.0	3,017 ±124	10,294 ±424	0.53 ±0.01	894	3.4 ±0.1	11.5 ±0.5	0.98	1.05	1.02	1.02	0.91
21.8	71.2	18.1	64.7	16.2	61.2	29.4	85.0	978.3	2,812 ±123	9,595 ±421	0.53 ±0.01	978	2.9 ±0.1	9.8 ±0.4	0.98	1.05	1.03	1.05	1.01
21.9	71.3	18.2	64.8	16.3	61.3	32.2	90.0	1012.0	2,724 ±123	9,294 ±420	0.53 ±0.01	1,012	2.7 ±0.1	9.2 ±0.4	0.99	1.05	1.03	1.03	1.01
21.8	71.3	18.1	64.7	16.2	61.2	35.0	95.0	1041.0	2,622 ±123	8,946 ±419	0.53 ±0.01	1,041	2.5 ±0.1	8.6 ±0.4	0.99	1.05	1.03	1.03	1.00
21.8	71.2	18.1	64.6	16.2	61.1	43.3	110.0	1139.0	2,344 ±123	7,998 ±419	0.53 ±0.01	1,139	2.1 ±0.1	7.0 ±0.4	0.99	1.05	1.03	1.04	1.01
26.6	79.8	13.7	56.7	2.5	36.5	20.8	69.5	842.5	2,718 ±110	9,274 ±377	0.93 ±0.02	843	3.2 ±0.1	11.0 ±0.5	0.98	1.05	1.02	1.02	0.61
26.7	80.1	13.8	56.8	2.4	36.3	29.6	85.3	947.6	2,530 ±109	8,632 ±372	0.94 ±0.02	948	2.7 ±0.1	9.1 ±0.4	0.98	1.05	1.03	1.04	0.60
26.7	80.1	13.9	57.0	2.7	36.9	32.2	90.0	980.2	2,457 ±109	8,383 ±371	0.94 ±0.02	980	2.5 ±0.1	8.6 ±0.4	0.98	1.05	1.03	1.04	0.98
26.8	80.2	14.0	57.2	3.1	37.5	35.0	95.1	1014.0	2,394 ±109	8,168 ±373	0.94 ±0.02	1,014	2.4 ±0.1	8.1 ±0.4	0.98	1.05	1.03	1.04	0.97
26.8	80.2	14.2	57.6	3.8	38.9	43.3	110.0	1124.0	2,157 ±109	7,360 ±373	0.94 ±0.02	1,124	1.9 ±0.1	6.5 ±0.3	0.97	1.06	1.03	1.04	0.97

Table 15. Steady-State Experimental Test Data for the Frigidaire FRA106CV1

Return DB		Return WB		Return DP		Outdoor DB		Fan Speed	Total Capacity		SHR	Total Power	COP	EER (Btu/Wh)	Balances				
(°C)	(°F)	(°C)	(°F)	(°C)	(°F)	(°C)	(°F)		(W)	(Btu/h)		(W)			$\varepsilon_{M,evap}$	$\varepsilon_{M,cond}$	$\varepsilon_{M,total}$	ε_{E}	ε_{W}
26.7	80.1	19.8	67.6	16.3	61.3	22.1	71.8	Med	3,254 ±134	11,103 ±456	0.60 ±0.01	707	4.6 ±0.2	15.7 ±0.7	0.99	1.03	1.02	1.00	1.04
26.7	80.1	19.8	67.7	16.4	61.5	29.4	84.9	Med	3,123 ±133	10,656 ±453	0.60 ±0.01	799	3.9 ±0.2	13.3 ±0.6	0.98	1.04	1.02	1.00	1.04
26.7	80.0	19.7	67.5	16.2	61.1	32.2	90.0	Med	3,038 ±132	10,366 ±450	0.62 ±0.01	834	3.6 ±0.2	12.4 ±0.6	0.98	1.04	1.02	1.00	1.04
26.7	80.0	19.8	67.6	16.3	61.3	35.0	95.0	Low	2,931 ±129	10,001 ±440	0.61 ±0.01	872	3.4 ±0.2	11.5 ±0.5	0.98	1.03	1.01	1.00	1.03
26.7	80.1	19.7	67.4	16.1	61.1	35.0	95.0	Med	2,939 ±131	10,028 ±447	0.62 ±0.01	873	3.4 ±0.2	11.5 ±0.5	0.98	1.04	1.02	1.00	1.05
26.8	80.2	19.6	67.2	15.9	60.6	35.0	94.9	High	3,006 ±155	10,256 ±529	0.66 ±0.02	933	3.2 ±0.2	11.0 ±0.6	0.99	1.03	1.01	1.01	1.04
26.7	80.1	19.6	67.3	16.0	60.7	43.3	109.9	Med	2,619 ±129	8,936 ±439	0.65 ±0.01	981	2.7 ±0.1	9.1 ±0.5	0.98	1.04	1.02	1.00	1.05
23.3	74.0	18.5	65.3	16.0	60.8	21.1	69.9	Med	3,075 ±132	10,492 ±449	0.55 ±0.01	715	4.3 ±0.2	14.7 ±0.7	0.98	1.03	1.01	0.99	1.01
23.3	73.9	18.4	65.2	15.9	60.5	29.5	85.2	Med	2,973 ±131	10,144 ±445	0.56 ±0.01	805	3.7 ±0.2	12.6 ±0.6	0.98	1.04	1.02	1.00	1.02
23.3	73.9	18.5	65.3	16.0	60.7	32.2	90.0	Med	2,898 ±130	9,888 ±444	0.56 ±0.01	841	3.4 ±0.2	11.8 ±0.6	0.98	1.04	1.02	0.99	1.02
23.3	73.9	18.6	65.4	16.1	61.0	35.0	95.0	Med	2,850 ±130	9,724 ±443	0.55 ±0.01	867	3.3 ±0.2	11.2 ±0.5	0.98	1.04	1.02	1.00	1.02
23.3	73.9	18.4	65.2	15.9	60.6	43.4	110.2	Med	2,547 ±128	8,690 ±436	0.57 ±0.01	971	2.6 ±0.1	8.9 ±0.5	0.98	1.05	1.02	0.99	1.04
21.2	70.2	17.6	63.7	15.7	60.2	21.1	70.0	Med	3,048 ±129	10,400 ±439	0.53 ±0.01	713	4.3 ±0.2	14.6 ±0.7	0.98	1.04	1.02	1.00	1.02
21.5	70.6	17.9	64.2	16.0	60.8	29.4	85.0	Med	2,928 ±128	9,990 ±437	0.53 ±0.01	803	3.6 ±0.2	12.5 ±0.6	0.98	1.05	1.02	1.00	1.03
21.5	70.7	17.9	64.3	16.0	60.9	32.2	90.0	Med	2,854 ±127	9,738 ±434	0.53 ±0.01	837	3.4 ±0.2	11.6 ±0.6	0.98	1.04	1.02	1.00	1.03
21.5	70.8	18.0	64.3	16.1	60.9	35.0	95.0	Med	2,775 ±127	9,468 ±433	0.53 ±0.01	866	3.2 ±0.2	10.9 ±0.5	0.98	1.04	1.02	1.00	1.03
21.5	70.7	17.8	64.1	15.9	60.6	43.3	110.0	Low	2,466 ±124	8,414 ±422	0.53 ±0.01	958	2.6 ±0.1	8.8 ±0.5	0.99	1.04	1.02	1.01	1.04
21.6	70.9	18.0	64.5	16.2	61.1	43.3	110.0	Med	2,506 ±128	8,550 ±436	0.52 ±0.01	961	2.6 ±0.1	8.9 ±0.5	0.98	1.04	1.02	1.00	1.04
21.2	70.1	17.7	63.8	15.8	60.4	43.4	110.1	High	2,532 ±148	8,639 ±506	0.53 ±0.01	1,004	2.5 ±0.2	8.6 ±0.5	1.00	1.03	1.02	1.02	1.03
26.7	80.0	13.4	56.1	1.3	34.4	20.0	68.1	Med	2,715 ±115	9,264 ±391	0.96 ±0.01	791	3.4 ±0.2	11.7 ±0.6	0.97	1.04	1.01	0.97	1.03
26.7	80.0	13.4	56.0	1.1	34.0	29.5	85.0	Med	2,481 ±112	8,465 ±382	0.96 ±0.02	885	2.8 ±0.1	9.6 ±0.5	0.97	1.04	1.02	0.97	1.04
26.8	80.2	13.4	56.2	1.2	34.1	32.3	90.1	Med	2,408 ±111	8,216 ±378	0.97 ±0.02	920	2.6 ±0.1	8.9 ±0.4	0.97	1.04	1.02	0.97	1.04
26.8	80.3	13.4	56.1	1.0	33.8	35.0	95.1	Med	2,342 ±111	7,991 ±378	0.97 ±0.02	950	2.5 ±0.1	8.4 ±0.4	0.98	1.04	1.02	0.98	1.05
26.8	80.3	13.6	56.4	1.7	35.0	43.3	110.0	Med	2,079 ±108	7,094 ±370	0.97 ±0.02	1,041	2.0 ±0.1	6.8 ±0.4	0.98	1.04	1.02	0.98	1.05

Table 16. Steady State Experimental Test Data for the Haier HWR-5XCL

Return DB		Return WB		Return DP		Outdoor DB		Fan Speed	Total Capacity		SHR	Total Power	COP	EER (Btu/Wh)	Balances				
(°C)	(°F)	(°C)	(°F)	(°C)	(°F)	(°C)	(°F)		(W)	(Btu/h)		(W)			$\varepsilon_{M,evap}$	$\varepsilon_{M,cond}$	$\varepsilon_{M,total}$	ε_{E}	ε_{W}
26.7	80.1	19.5	67.1	18.3	64.9	20.5	68.9	Med	1,582 ±58	5,398 ±198	0.61 ±0.01	437	3.6 ±0.1	12.4 ±0.4	1.00	0.99	1.00	1.00	1.02
26.7	80.0	19.5	67.1	18.4	65.1	29.4	84.9	Med	1,487 ±57	5,074 ±195	0.61 ±0.01	504	2.9 ±0.1	10.1 ±0.4	1.00	1.00	1.00	1.02	1.02
26.7	80.1	19.5	67.2	18.4	65.2	32.2	89.9	Med	1,443 ±57	4,924 ±194	0.61 ±0.01	525	2.7 ±0.1	9.4 ±0.4	0.99	1.01	1.00	1.02	1.01
26.7	80.0	19.7	67.5	19.0	66.2	35.0	94.9	Low	1,323 ±52	4,514 ±178	0.60 ±0.01	552	2.4 ±0.1	8.2 ±0.3	0.99	0.99	0.99	1.01	1.01
26.7	80.1	19.6	67.3	18.5	65.2	35.0	95.0	Med	1,397 ±57	4,767 ±193	0.62 ±0.01	545	2.6 ±0.1	8.8 ±0.3	0.99	1.01	1.00	1.02	1.01
26.7	80.0	19.5	67.2	18.6	65.4	35.0	95.1	High	1,447 ±62	4,937 ±213	0.63 ±0.01	548	2.6 ±0.1	9.0 ±0.4	1.00	0.99	0.99	1.01	1.02
26.7	80.1	19.6	67.3	18.6	65.4	43.3	110.0	Med	1,238 ±55	4,224 ±189	0.63 ±0.01	602	2.1 ±0.1	7.0 ±0.3	1.00	1.01	1.00	1.03	1.02
23.3	73.9	18.7	65.6	18.1	64.6	20.6	69.1	Med	1,545 ±57	5,272 ±196	0.54 ±0.01	431	3.6 ±0.1	12.2 ±0.4	1.00	0.99	1.00	0.99	1.02
23.1	73.6	18.4	65.1	18.1	64.6	29.4	84.9	Med	1,459 ±56	4,978 ±192	0.55 ±0.01	485	3.0 ±0.1	10.3 ±0.4	1.00	1.00	1.00	1.01	1.02
22.8	73.1	18.2	64.7	18.1	64.5	32.2	90.0	Med	1,393 ±56	4,753 ±190	0.55 ±0.01	502	2.8 ±0.1	9.5 ±0.4	1.00	1.00	1.00	1.01	1.02
23.0	73.4	18.3	64.9	18.2	64.7	35.0	95.0	Med	1,351 ±55	4,610 ±188	0.55 ±0.01	520	2.6 ±0.1	8.9 ±0.4	1.00	1.00	1.00	1.01	1.02
23.1	73.5	18.3	64.9	18.2	64.7	43.3	109.9	Med	1,191 ±54	4,064 ±184	0.56 ±0.01	577	2.1 ±0.1	7.0 ±0.3	1.00	1.01	1.01	1.03	1.02
20.9	69.7	17.7	63.8	18.0	64.4	21.0	69.8	Med	1,516 ±57	5,173 ±193	0.52 ±0.01	428	3.5 ±0.1	12.1 ±0.4	1.00	0.99	1.00	1.00	1.02
21.0	69.9	17.7	63.9	17.8	64.0	29.4	84.9	Med	1,443 ±56	4,924 ±191	0.52 ±0.01	473	3.0 ±0.1	10.4 ±0.4	0.99	1.01	1.00	1.02	1.02
21.0	69.8	17.7	63.9	17.9	64.2	32.2	90.0	Med	1,389 ±55	4,739 ±189	0.52 ±0.01	497	2.8 ±0.1	9.5 ±0.4	1.00	1.00	1.00	1.01	1.02
21.1	69.9	17.8	64.0	18.1	64.5	35.0	95.0	Med	1,345 ±55	4,589 ±188	0.52 ±0.01	514	2.6 ±0.1	8.9 ±0.4	1.00	1.01	1.00	1.02	1.01
21.3	70.3	18.0	64.3	18.3	64.9	43.3	110.0	Med	1,189 ±54	4,057 ±184	0.52 ±0.01	569	2.1 ±0.1	7.1 ±0.3	0.99	1.01	1.01	1.03	1.02
26.7	80.0	15.4	59.7	-2.4	27.7	21.0	69.9	Med	1,330 ±51	4,538 ±175	0.86 ±0.01	455	2.9 ±0.1	10.0 ±0.4	0.97	1.02	1.00	1.03	1.10
26.7	80.0	15.4	59.7	-2.2	28.0	29.4	84.9	Med	1,203 ±51	4,105 ±173	0.89 ±0.02	516	2.3 ±0.1	8.0 ±0.3	0.98	1.02	1.01	1.05	1.00
26.6	79.9	15.2	59.4	-2.2	28.1	32.2	90.0	Med	1,150 ±51	3,924 ±172	0.91 ±0.02	533	2.2 ±0.1	7.4 ±0.3	0.98	1.02	1.01	1.05	0.96
26.7	80.1	15.2	59.3	-2.2	28.1	35.0	95.0	Med	1,112 ±50	3,794 ±172	0.93 ±0.02	553	2.0 ±0.1	6.9 ±0.3	0.98	1.02	1.00	1.05	0.93
26.7	80.1	15.1	59.2	-2.1	28.2	43.3	109.9	Med	1,007 ±49	3,436 ±169	0.94 ±0.02	614	1.6 ±0.1	5.6 ±0.3	0.99	1.01	1.00	1.05	0.81

Table 17. Steady State Experimental Test Data for the GE AGD06LAG1

Return DB		Return WB		Return DP		Outdoor DB		Fan Speed	Total Capacity		SHR	Total Power	COP	EER (Btu/Wh)	Balances				
(°C)	(°F)	(°C)	(°F)	(°C)	(°F)	(°C)	(°F)		(W)	(Btu/h)		(W)			$\varepsilon_{M,evap}$	$\varepsilon_{M,cond}$	$\varepsilon_{M,total}$	ε_{E}	ε_{W}
26.7	80.1	13.5	56.3	1.5	34.7	27.8	82.1	Med	743 ±85	2,535 ±290	1.00 ±0.00	460	1.6 ±0.1	5.5 ±0.3	1.00	1.01	1.00	1.03	1.00
23.1	73.5	18.6	65.5	16.3	61.4	32.2	90.0	Med	1,018 ±66	3,473 ±224	0.57 ±0.02	758	1.3 ±0.1	4.6 ±0.3	0.98	1.01	0.99	1.03	0.98
23.0	73.5	18.6	65.4	16.2	61.2	35.0	95.0	Med	970 ±64	3,310 ±220	0.59 ±0.02	776	1.3 ±0.1	4.3 ±0.3	0.99	1.01	0.99	1.03	0.98
22.9	73.2	18.4	65.1	16.0	60.8	43.3	109.9	Med	770 ±60	2,627 ±204	0.63 ±0.02	836	0.9 ±0.1	3.1 ±0.2	0.98	1.01	1.00	1.04	0.97
21.7	71.0	17.2	63.0	14.7	58.4	19.1	66.3	Med	1,095 ±72	3,736 ±246	0.61 ±0.01	573	1.9 ±0.1	6.5 ±0.3	0.99	0.99	0.99	1.01	0.95
21.9	71.3	17.5	63.5	15.1	59.1	29.4	84.9	Med	972 ±66	3,316 ±225	0.61 ±0.02	679	1.4 ±0.1	4.9 ±0.3	0.99	1.00	0.99	1.04	0.97
21.8	71.3	17.4	63.4	15.0	59.0	32.2	89.9	Med	921 ±64	3,144 ±219	0.62 ±0.02	702	1.3 ±0.1	4.5 ±0.3	0.99	1.00	0.99	1.04	0.97
21.8	71.3	17.5	63.4	15.0	59.1	35.0	95.0	Med	881 ±63	3,004 ±215	0.62 ±0.02	722	1.2 ±0.1	4.2 ±0.3	0.99	1.00	0.99	1.05	0.97
21.8	71.3	17.5	63.4	15.0	59.0	43.3	110.0	Med	716 ±58	2,442 ±199	0.67 ±0.02	769	0.9 ±0.1	3.2 ±0.2	0.99	1.00	1.00	1.06	0.96
26.7	80.1	13.5	56.3	1.5	34.8	21.1	70.0	Med	878 ±103	2,997 ±351	1.00 ±0.00	402	2.2 ±0.1	7.5 ±0.3	0.99	1.02	1.00	1.08	0.99
26.7	80.1	13.3	56.0	1.0	33.8	29.4	84.9	Med	724 ±88	2,470 ±302	1.00 ±0.00	433	1.7 ±0.1	5.7 ±0.3	0.99	1.02	1.00	1.07	0.99
26.8	80.2	19.7	67.4	16.1	60.9	21.1	70.0	Med	1,266 ±70	4,320 ±240	0.66 ±0.02	670	1.9 ±0.1	6.4 ±0.3	0.99	1.00	0.99	1.01	0.95
26.7	80.1	13.3	56.0	1.0	33.8	32.2	89.9	Med	674 ±84	2,299 ±285	1.00 ±0.00	445	1.5 ±0.1	5.2 ±0.2	1.00	1.01	1.00	1.06	1.00
26.7	80.1	13.3	55.9	0.9	33.5	35.0	95.1	Med	622 ±80	2,121 ±271	1.00 ±0.00	447	1.4 ±0.1	4.7 ±0.2	1.00	1.01	1.00	1.06	1.00
26.7	80.1	13.4	56.1	1.2	34.1	43.3	110.0	Med	478 ±69	1,630 ±236	1.00 ±0.00	432	1.1 ±0.1	3.8 ±0.2	1.00	1.01	1.01	1.07	1.00
26.8	80.3	19.6	67.4	16.0	60.8	29.4	84.9	Med	1,138 ±67	3,883 ±230	0.67 ±0.02	752	1.5 ±0.1	5.2 ±0.3	0.99	1.00	0.99	1.03	0.96
26.7	80.0	19.6	67.2	16.0	60.7	32.2	90.0	Med	1,080 ±66	3,685 ±226	0.68 ±0.02	784	1.4 ±0.1	4.7 ±0.3	0.99	1.00	0.99	1.03	0.97
26.6	79.9	19.5	67.2	15.9	60.6	35.0	95.0	Med	1,025 ±65	3,497 ±222	0.70 ±0.02	806	1.3 ±0.1	4.3 ±0.3	0.99	1.00	1.00	1.04	0.97
26.8	80.2	19.6	67.2	15.9	60.6	43.3	110.0	Med	843 ±2	2,876 ±6	0.78 ±0.03	886	1.0 ±0.1	3.2 ±0.2	0.99	1.01	1.00	1.05	0.99
23.0	73.5	18.7	65.6	16.4	61.5	21.1	70.0	Med	1,200 ±71	4,094 ±241	0.55 ±0.01	638	1.9 ±0.1	6.4 ±0.3	0.99	1.00	0.99	1.01	0.98
23.0	73.4	18.6	65.5	16.3	61.4	29.4	84.9	Med	1,079 ±67	3,682 ±230	0.57 ±0.01	720	1.5 ±0.1	5.1 ±0.3	0.98	1.00	0.99	1.03	0.98

Appendix C: Normalized Temperature Performance Curves

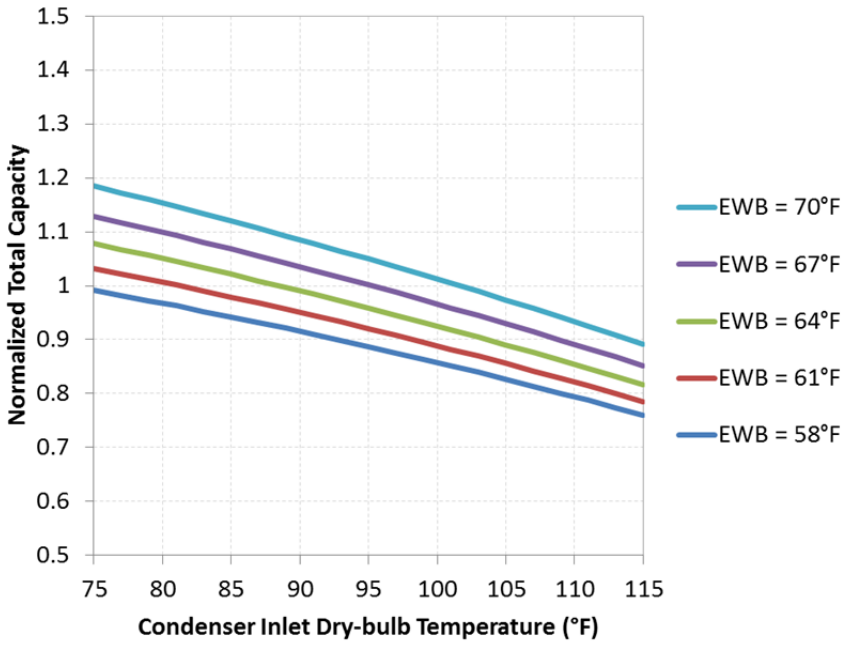

Figure 34. Normalized total capacity temperature-based performance curves for the Frigidaire FRA103BT1

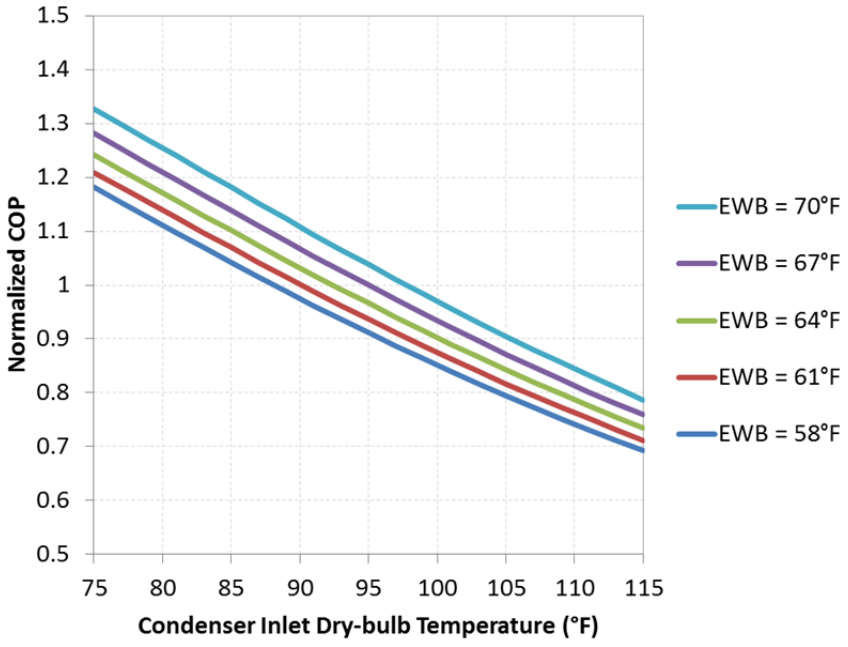

Figure 35. Normalized COP (1/EIR) temperature-based performance curves for the Frigidaire FRA103BT1

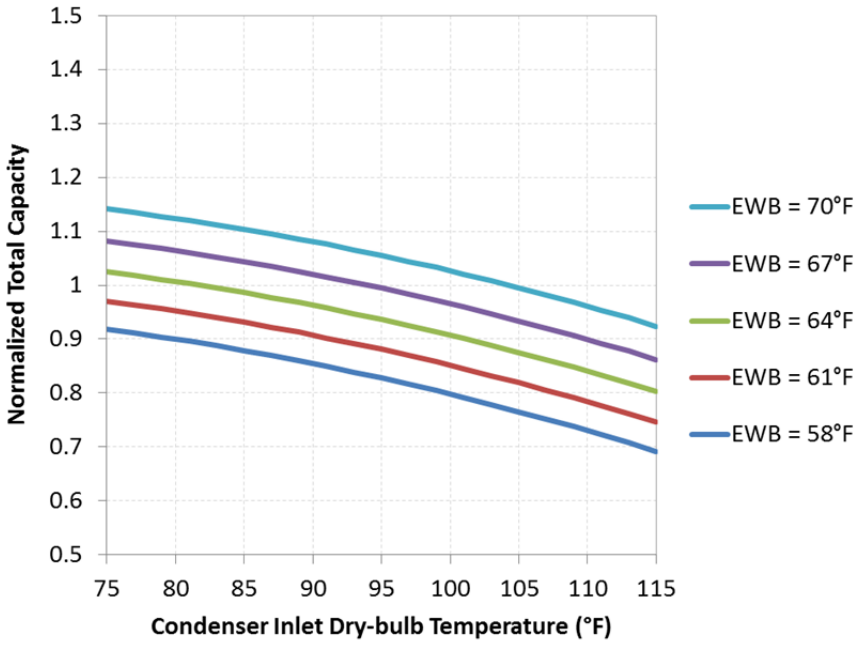

Figure 36. Normalized total capacity temperature-based performance curves for the Frigidaire FRA106CV1

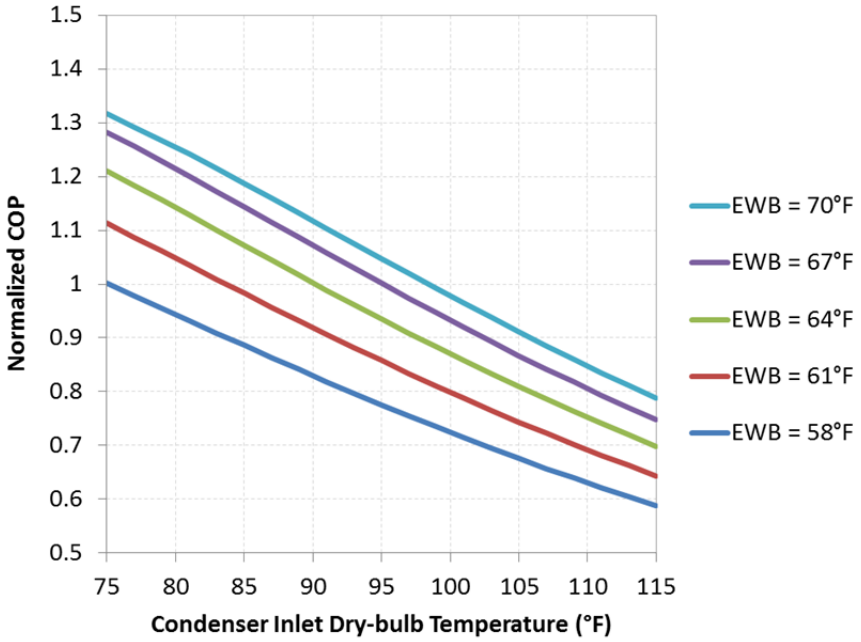

Figure 37. Normalized COP (1/EIR) temperature-based performance curves for the Frigidaire FRA106CV1

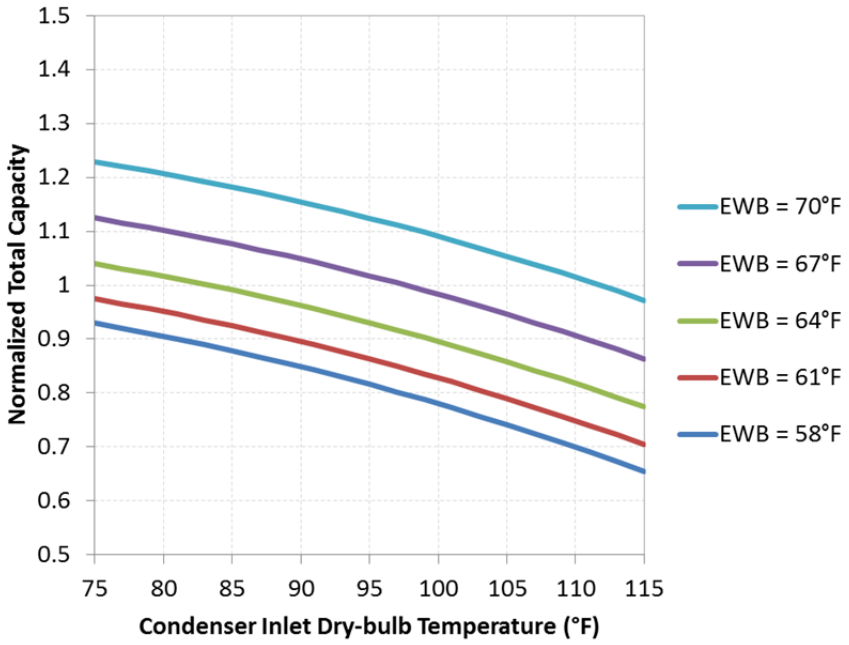

Figure 38. Normalized total capacity temperature-based performance curves for the Haier HWR-5XCL

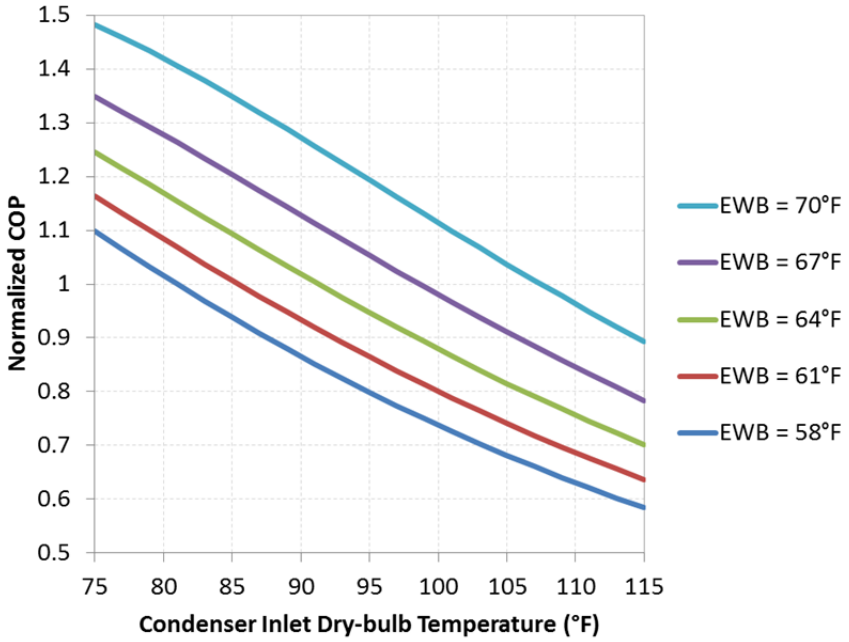

Figure 39. Normalized COP (1/EIR) temperature-based performance curves for the Haier HWR-5XCL

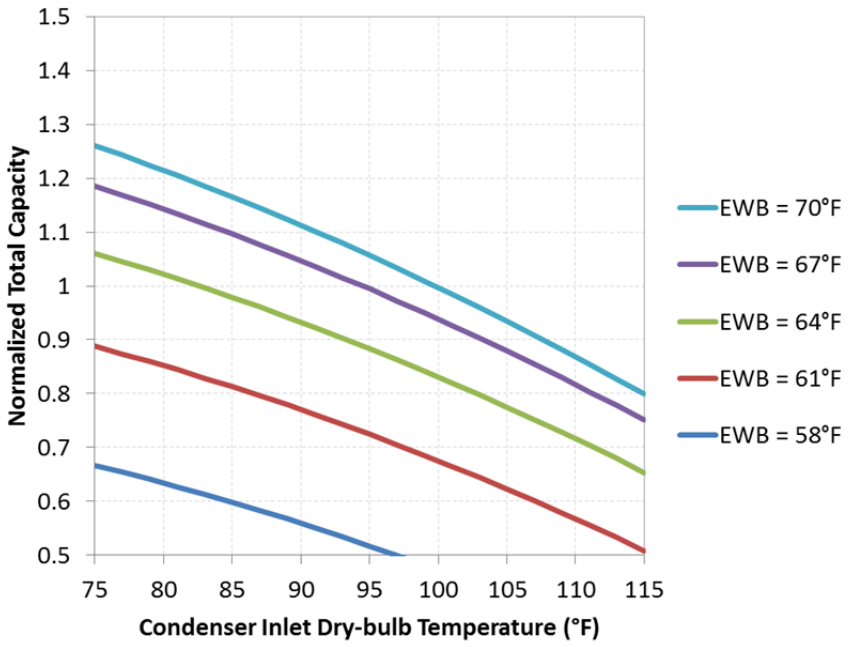

Figure 40. Normalized total capacity temperature-based performance curves for the GE AGD06LAG1

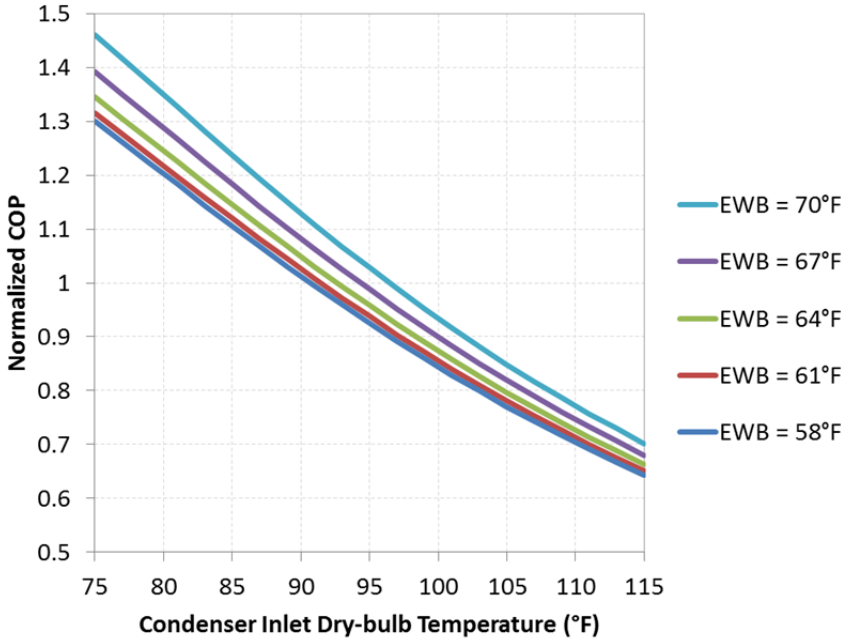

Figure 41. Normalized COP (1/EIR) temperature-based performance curves for the GE AGD06LAG1

Appendix D: Normalized Flow Fraction Performance Curves

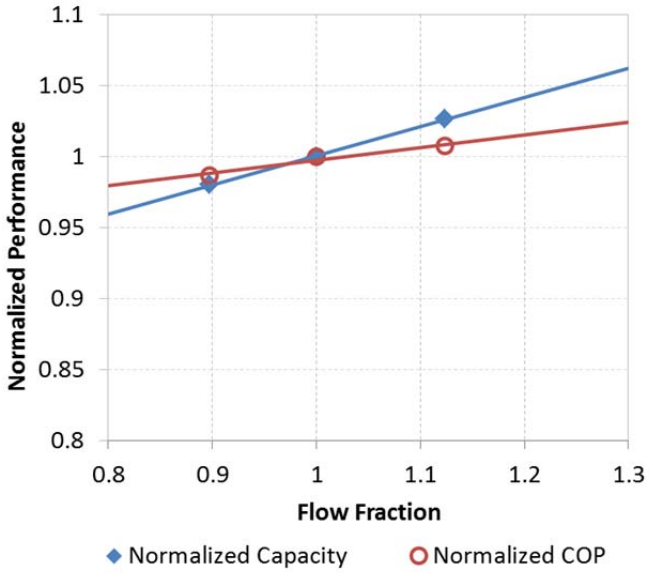

Figure 42. Normalized flow fraction performance curves for the Frigidaire FRA103BT1

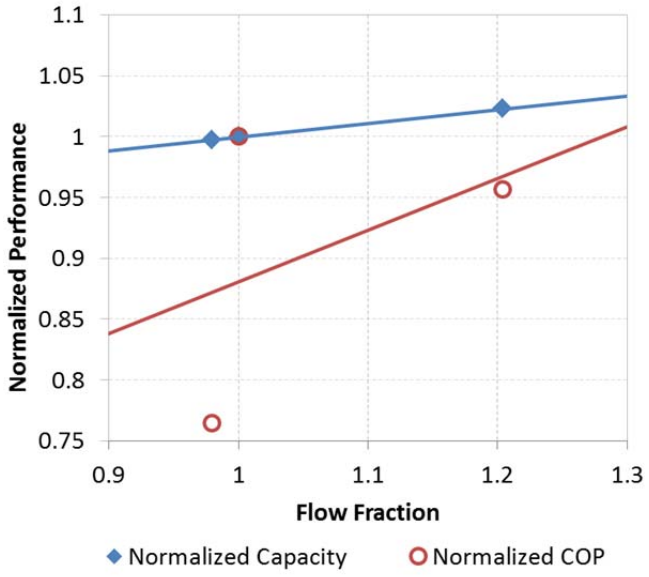

Figure 43. Normalized flow fraction performance curves for the Frigidaire FRA106CV1

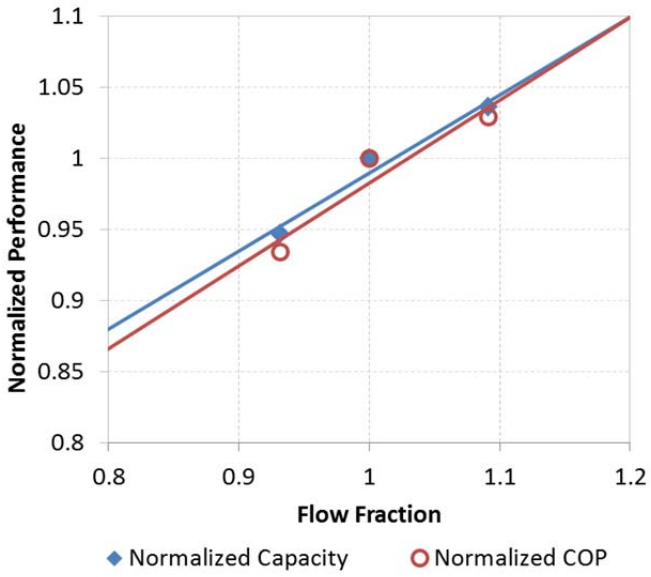

Figure 44. Normalized flow fraction performance curves for the Haier HWR-5XCL